Pion and kaon polarizabilities in the quark confinement model

M. A. Ivanov
Department of Physics, Virginia Polytechnic Institute and State University, Blacksburg, Virginia 24061
*and Laboratory of Theoretical Physics, Joint Institute for Nuclear Research, Head Post Office P.O.Box 79, 101000 Moscow, U.S.S.R.**

T. Mizutani
Centro de Física Nuclear da Universidade de Lisboa, Avenida Gama Pinto 2, P-1699 Lisboa Codex, Portugal
*and Department of Physics, Virginia Polytechnic Institute and State University, Blacksburg, Virginia 24061**
(Received 09 May 1991)

The Dubna quark confinement model is applied to the study of electromagnetic polarizabilities of the π and K mesons. Within this model it is found that the effect of quark confinement reduces the value of the pion polarizability from that obtained in such approaches as chiral quark loop and linear σ models. In the chiral limit our result coincides with the one found in chiral perturbation theory. For the charged kaon we find the electric polarizability considerably larger than the chiral prediction. This is due to the strong meson-mass dependence not expected from the pointlike interaction in effective meson Lagrangian approaches.

PACS number(s): 13.40.Fn, 12.40.Aa, 13.60.Fz, 14.40.Aq

I. INTRODUCTION

The electric and magnetic polarizabilities of hadrons are two basic parameters which, together with their electric charges and masses, characterize the low energy photon-hadron amplitudes. In this respect these quantities must be considered as fundamental as electromagnetic mean square radii, static magnetic moments, etc., and are expected to give us useful information on the internal structure of hadrons. See the several review articles [1–4]. Our interest here is the electromagnetic polarizabilities of the pion and kaon.

As is well known, these mesons are members of the pseudoscalar octet which is characterized by its *Goldstone* nature: they emerge from the spontaneous breaking of the $SU(3)_L \times SU(3)_R$ chiral symmetry to $SU(3)_V$. At this stage all members of this octet are massless. In reality, they acquire finite masses due to the explicit breaking of chiral symmetry caused by the nonzero current quark masses. This breaking is small for the pion, resulting in its very small physical mass (on the hadronic scale), but is not quite so for the kaon. The consequence is that when one wants to calculate any quantity associated with the low-energy pion (kaon), one must adopt a theoretical model which respects the (spontaneously broken) chiral symmetry. The study of the electromagnetic polarizability of the pion and kaon that we are interested in just falls into this category.

Theoretical investigation in this subject (mostly on the pion electromagnetic polarizabilities) has been pursued since the early 1970s [5–11] by employing various models embodying chiral symmetry: current algebra + PCAC (partial conservation of axial-vector current) [5], the linear σ model and its variants [8, 9], the nonlinear σ model [10], etc. In the exact chiral limit where the mass of the pion vanishes, one found (independently of the model difference) the following relations between the α_π (electric) and β_π (magnetic) polarizabilities:

$$\alpha_\pi + \beta_\pi = 0, \quad \alpha_{\pi^0} = 0,$$

when the effect of the pion loop was not considered for the latter. Some models [6, 9] took into account corrections arising from the nonvanishing pion mass, while others [8, 10] included the effect of the pion and even the baryon loops. With those corrections,

$$\alpha_{\pi^0} \sim \frac{1}{10}\alpha_{\pi^\pm},$$

but often with a negative sign relative to the charged-pion polarizability. Furthermore, all the models except one predicted a value of the electric polarizability within the range

$$4.0 \times 10^{-43} \leq \alpha_{\pi^\pm} \leq 6.0 \times 10^{-43}\ \text{cm}^3,$$

in Gaussian units. We note that models not based upon a chiral Lagrangian, i.e., dispersion relations and finite-energy sum rules, also obtained the polarizability within this range of values [12, 13]. In the rest of our discussion we shall call these models and/or their results large-valued results (LVR's).

The exception to LVR's is the current algebra + PCAC approach of Terent'ev [5], which related the polarizability

*Permanent address.

to the ratio, $\gamma \equiv h_A(0)/h_V(0)$, of the vector and axial-vector form factors in radiative pion decay $\pi \to \gamma e\nu$. For $\gamma \sim 0.46$ from recent data [14], one finds

$$\alpha_{\pi^\pm} \sim 2.8 \times 10^{-43}\ \mathrm{cm}^3,$$

which is roughly a factor of 2 smaller than LVR's.

In the meantime, this quantity was deduced from radiative pion-nucleus scattering [15] to be

$$\alpha_{\pi^\pm} = (6.8 \pm 1.4_{\mathrm{stat}} \pm 1.8_{\mathrm{syst}}) \times 10^{-43}\ \mathrm{cm}^3,$$

with the assumption $\alpha_\pi + \beta_\pi = 0$, and

$$\beta_{\pi^\pm} = [-7.1 \pm 2.8(\mathrm{stat}) \pm 1.8(\mathrm{syst}) \times 10^{-43}\ \mathrm{cm}^3,$$

$$\alpha_{\pi^\pm} + \beta_{\pi^\pm} = [1.4 \pm 3.1(\mathrm{stat}) \pm 2.5(\mathrm{syst})] \times 10^{-43}\ \mathrm{cm}^3,$$

without the above assumption. Apparently this result is consistent with LVR's but not with the result of Terent'ev.

Recently, there has been extensive work in the low-energy realization of quantum chromodynamics (QCD) called chiral perturbation theory (CHPT) [16], in which the QCD partition functional with external sources is represented in terms of a nonlinear realization of chiral symmetry. In particular, it was shown that the low-energy effective Lagrangian for the basic pseudoscalar octet may be systematically constructed in inverse powers of $(4\pi F_\pi)^2$, where F_π (= 93.3 MeV) is the pion decay constant, or equivalently, in powers of the external momentum squared p^2 and the meson (or quark) masses. The leading order, conventionally denoted as $\mathcal{L}_2$, is nothing but a nonlinear σ model. The next order, $\mathcal{L}_4 = O(1/(4\pi F_\pi)^2)$, contains several parameters. By adjusting these empirically, this theoretical model has been very successful in correlating a large body of low-energy quantities as well as in giving accurate predictions. We note that there have been interesting attempts in deriving these parameters by integrating the non-Abelian axial anomaly in the QCD Lagrangian, see for example [17].

CHPT was applied to the pion polarizability by Donoghue and Holstein [18]. Its prediction for $\alpha_{\pi^\pm}$ was in perfect agreement with that by Terent'ev [5], thus smaller than the experimental result [15] and LVR's by about a factor of 2. In view of the complete consistency between current algebra + PCAC and the effective Lagrangian in CHPT [at least up to $O(p^4)$], the agreement of these two model predictions may not be a surprise. To simplify our discussion we call these predictions small-valued results (SVR's) in what follows.

Donoghue and Holstein then argued that approaches like linear σ models, which predict large values for the charged pion polarizability, viz., LVR's, are not trustworthy in view of their poor prediction on the coefficients in the $\mathcal{L}_4$ contribution. To test their prediction, they urged experimentalists to remeasure α_π.

It is this apparent conflict between the data and the most recent (and supposedly most reliable) CHPT prediction that has motivated us to study this subject from a somewhat different angle. Our theoretical basis is the *quark confinement model* (QCM) developed at Dubna [19]. Like the effective Lagrangian of CHPT, this model may be inferred from the study of QCD partition functionals. But in QCM the implementation of chiral symmetry is not the main guiding principle; rather, the emphasis is placed on quark confinement and the composite nature of hadrons, with the aspect of chiral symmetry imposed later. We think that at least one merit of the present approach is the possibility to handle more easily the situations where chiral symmetry breaking is strong. This should then facilitate the calculation of the electromagnetic polarizabilities of the kaon, the mass of which may not really be regarded as vanishingly small in the low-energy domain of our present interest.

We should mention that QCM has already been applied to the pion polarizability problem [20]. However, the authors were not informed of the result of Ref. [18] and, thus, not much aware of the conflict discussed above. In addition, to simplify the calculation, contributions involving quark loops were evaluated with a vanishing mass for the external pions. One cannot apply this work directly to the kaon polarizability where the finite-mass effect is expected to be important. Furthermore, there are some errors which are rather serious. So here, we carefully correct and extend this previous work.

Our principal findings may be summarized as follows.

(1) For charged pions, $\alpha_{\pi^\pm} \sim 3.6 \times 10^{-43}\ \mathrm{cm}^3$, which is smaller than LVR's, but larger than SVR's. Particularly in the exact chiral limit our result practically coincides with the latter. We attribute the origin of our lower value (than LVR) to the effect of quark confinement.

(2) For charged mesons, quark loop contributions have a strong mass dependence, which may not be inferred easily from other existing models. As a consequence, the charged kaon polarizability becomes considerably larger than what chiral models predict. This gives us hope that it may be measured experimentally without much difficulty.

This article is organized as follows. Section II gives a brief account of the QCM applied to our present calculation. In Sec. III we first outline how the electromagnetic polarizability of a scalar (or pseudoscalar) particle may be extracted from the Compton amplitude. Then we present the invariant Compton amplitude from our model, and the polarizabilities extracted from it. Some details of the calculation of the amplitude as well as definitions of certain functions appearing in this section are relegated to the Appendixes. Finally, Sec. IV is devoted to presenting our numerical results and discussions in comparison with other model predictions. In order to minimize the shuttling back and forth between this and other related articles, we have tried to make this article as pedagogical and self-contained as possible, except for Sec. II where, to contain the size of this section, only some rudiments of the QCM necessary for our present objective are presented.

II. THE QUARK STRUCTURE OF MESONS IN QCM

In the present section we give a brief account of the Dubna quark confinement model (QCM) which is employed in the present study of meson electromagnetic

polarizabilities. A particular emphasis is placed on how to describe the scalar-meson sector. A similar approach originating from a chiral-invariant four-quark interaction to arrive at a generalized σ model (often called the superconducting-type model) may be noted [21]. However, the aspect of quark confinement is not considered therein.

A heuristic bosonization procedure starting from the QCD generating functional is the basis of our meson-quark interaction Lagrangian in the QCM. Since our present objective is the application of this Lagrangian to actual physical problems, we refer the interested reader to Ref. [19]. There he (or she) will find how our Lagrangian may be reached within this type of approach.

The interaction Lagrangian for the meson octet Φ_i is written as

$$L_M = \frac{g_M}{\sqrt{2}} \sum_{i=1}^{8} \Phi_i \bar{q} \Gamma_M \lambda_i q. \tag{1}$$

Here, λ_i (i=1,...,8) are the Gell-Mann matrices ($\lambda_0 = \sqrt{2/3} I$), and Γ_M are the Dirac matrices: $i\gamma^5$ for pseudoscalar $P(\pi, K, \eta, \eta')$; γ^μ for vector $V(\rho, K^*, \omega, \phi)$; $\gamma^\mu\gamma^5$ for axial vector $A(a_1, K_1, f_1)$. For the coupling to scalar mesons $S(a_0, K_0, f_0, \varepsilon)$, our Γ_M takes a form which contains a derivative. It will be given where we discuss the QCM description of scalar mesons later in this section. The relation between the octet fields Φ_i and the physical meson fields (M's) together with the relevant flavor matrices is the standard one, and is listed in Table I. The difference between the actual and ideal singlet-octet mixing angles is denoted as δ_M (the ideal mixing angle is defined as $\cos\theta_I = \sqrt{2/3}$). For example, $\delta_V = 0°$ and $\delta_P = -46°$, are adopted for vector and pseudoscalar mesons, respectively. We shall discuss the value for the scalar mesons later.

In the QCM we assume that mesons are bound states of $q\bar{q}$, which is expressed in the *compositeness condition* that the renormalization constant for meson M is equal to zero:

$$Z_M = 1 + h_M \tilde{\Pi}'_M(m_M^2) = 0. \tag{2}$$

where $h_M = N_c g_M^2/(2\pi)^2$ with $N_c = 3$ is the effective coupling constant and $\tilde{\Pi}'_M(p^2)$ is the derivative of the (renormalized) meson-mass operator, see Appendix B and Fig. 1. Physically, this condition means that the probability to find the meson M in a bare state is equal to zero. It is important to remark here that (i) our interaction Lagrangian together with the compositeness condition has been shown to be equivalent to the one obtained by the QCD bosonization procedure [19], and (ii) the compositeness condition allows one to determine the coupling constant h_M (or g_M) as a function of the physical meson mass. In fact, meson masses are the input to our model.

Mesonic interactions in the QCM are defined by diagrams involving closed quark loops which can be obtained from the S matrix:

$$S = \int d\sigma_{\rm vac}\, T \exp\left(i \int dx\, L_M(x) \right). \tag{3}$$

Here, the T product is the ordinary Wick time ordering for the mesonic and quark fields. The quark propagator in the presence of the gluonic vacuum background $B_{\rm vac}$ has the form

$$\begin{aligned} S(x_1, x_2|B_{\rm vac}) &= <0|T[q(x_1)\bar{q}(x_2)]|0> \\ &= i(\not{p} + \not{B}_{\rm vac})^{-1}\delta(x_1 - x_2). \end{aligned} \tag{4}$$

We then assume [19] that an average over $B_{\rm vac}$ of the quark loops generated by the S matrix provides the quark confinement and make the theory ultraviolet finite. This averaging takes the form

$$\int d\sigma_{\rm vac}\, {\rm tr}[M(x_1)S(x_1x_2|B_{\rm vac}) \cdots M(x_n)S(x_nx_1|B_{\rm vac})], \tag{5}$$

where $\sigma_{\rm vac}$ is a set of variables characterizing $B_{\rm vac}$. Our confinement ansatz is then to replace this equation by

$$\int d\sigma_v\, {\rm tr}[M(x_1)S_v(x_1 - x_2) \cdots M(x_n)S_v(x_n - x_1)]. \tag{6}$$

Here,

TABLE I. SU(3) nonets. The names are from the recent Particle Data Group compilation.

S	T	T_3	Name (PDG) Ref. [14]	Physical field	Physical λ matrix
0	1	±1	$\pi^\pm, \rho^\pm, a_0^\pm, a_1^\pm$	$M^\pm = (\Phi^1 \mp i\Phi^2)/\sqrt{2}$	$\tilde{\lambda}^\mp = (\lambda^1 \pm i\lambda^2)/\sqrt{2}$
0	1	0	$\pi^0, \rho^0, a_0^0, a_1^0$	$M^0 = \Phi^3$	$\tilde{\lambda}^0 = \lambda^3$
1	$\frac{1}{2}$	$\frac{1}{2}$	$K^+, (K^*)^+, K_0^+, K_1^+$	$M_s^+ = (\Phi^4 - i\Phi^5)/\sqrt{2}$	$\tilde{\lambda}_s^- = (\lambda^4 + i\lambda^5)/\sqrt{2}$
1	$\frac{1}{2}$	$-\frac{1}{2}$	$K^0, (K^*)^0, K_0^0, K_1^0$	$M_s^0 = (\Phi^6 - i\Phi^7)/\sqrt{2}$	$\tilde{\lambda}_s^0 = (\lambda^6 + i\lambda^7)/\sqrt{2}$
−1	$\frac{1}{2}$	$\frac{1}{2}$	$\bar{K}^0, (\bar{K}^*)^0, \bar{K}_0^0, \bar{K}_1^0$	$\bar{M}_s^0 = (\Phi^6 + i\Phi^7)/\sqrt{2}$	$\tilde{\lambda}_s^0 = (\lambda^6 - i\lambda^7)/\sqrt{2}$
−1	$\frac{1}{2}$	$-\frac{1}{2}$	$K^-, (K^*)^-, K_0^-, K_1^-$	$M_s^- = (\Phi^4 + i\Phi^5)/\sqrt{2}$	$\tilde{\lambda}_s^+ = (\lambda^4 - i\lambda^5)/\sqrt{2}$
0	0	0	$\eta', \omega, \varepsilon, D$	$M' = \Phi^0\cos\theta - \Phi^8\sin\theta$	$\tilde{\lambda}_{M'} = -\lambda^8\sin\theta + \lambda^0\cos\theta$
0	0	0	η, ϕ, f_0, f_1	$M = \Phi^0\sin\theta + \Phi^8\cos\theta$	$\tilde{\lambda}_M = \lambda^8\cos\theta + \lambda^0\sin\theta$

$$\tilde{\lambda}_{M'} = {\rm diag}(\cos\delta, \cos\delta, -\sqrt{2}\sin\delta)$$
$$\tilde{\lambda}_M = {\rm diag}(-\sin\delta, -\sin\delta, -\sqrt{2}\cos\delta)$$
$$\delta = \theta - \theta_I, \quad \cos\theta_I = \sqrt{\tfrac{2}{3}}, \quad \theta_I = 35°26'$$

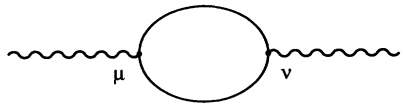

FIG. 1. Typical mass (or self-energy) operator.

$$S_v(x_1 - x_2) = \int \frac{d^4p}{(2\pi)^4 i} e^{-ip\cdot(x_1-x_2)} \frac{1}{v\Lambda - \not{p}} \tag{7}$$

is a quark propagator with the scale parameter Λ characterizing the size of the confinement (or it may be viewed as something equivalent to the constituent mass), and the measure $d\sigma_v$, which is essential for quark confinement, is defined to provide the absence of singularities in Eq. (7) corresponding to the physical quark production:

$$\int \frac{d\sigma_v}{v - z} \equiv G(z) = a(-z^2) + zb(-z^2). \tag{8}$$

We shall call $G(z)$ the confinement function. It is an entire analytic function which decreases faster than the inverse of any polynomial of z in a Euclidean direction $z^2 \to -\infty$. We further assume that $G(z)$ is a universal function, i.e., independent of color and flavor. In other words, $G(z)$ is common for all quark diagrams defining the hadron interaction at low energies. Otherwise, there is no other constraint on it. In practice, it has turned out [19] that low-energy physics depends only on those quantities which involve the integral of $a(u)$ and $b(u)$ together with u^N $(N = 0, 1, 2)$, but not on the detailed shape of these functions. We thus have made a simple choice:

$$a(u) = a_0 \exp(-u^2 - a_1 u), \quad b(u) = b_0 \exp(-u^2 + b_1 u). \tag{9}$$

The parameters a_i, b_i, and Λ have been determined from the best model description of data in low-energy processes. The following values are found:

$$a_0 = b_0 = 2, \quad a_1 = 1, \quad b_1 = 0.4, \quad \text{and } \Lambda = 460 \text{ MeV},$$

which describe various basic constants quite well, as found in Table II.

With these parameters fixed, one may be able to describe the basic characteristics of various mesons (see, for example, the second reference in [19]). Of particular interest in our present context is the success of the model in describing the pion electromagnetic form factor both in the spacelike and timelike regions. The corresponding mean-square radius is found to be

$$\langle r_\pi^2 \rangle = 0.43 \text{ fm}^2,$$

as compared with the data [22]:

$$\langle r_\pi^2 \rangle_{\text{expt}} = 0.44 \pm 0.03 \text{ fm}^2.$$

Agreement of the model prediction with experiments was however not reached in the scalar meson sector with a simple form of the scalar quark current: $\Gamma_M \propto \bar{q}q$ [20]. Since scalar mesons are essential ingredients in the context of our present study, we shall summarize and supplement here the issue discussed in [20].

Scalar mesons play an important role in low-energy physics, but are at the same time rather controversial both theoretically and experimentally. First, they facilitate the description of low-energy processes, especially in implementing chiral symmetry [23]; recall the linear σ model. Also, it is important, in the phenomenological studies of $\pi\pi, \pi N$, and NN scattering processes, to include intermediate scalar meson exchanges either in the s or t channels [23, 24]. The medium range attraction in the nucleon-nucleon potential is a good example in which the light scalar meson ε (or σ), with the mass of 600 – 700 MeV, is often introduced [24]. The problem is that to date this light scalar meson has not been confirmed experimentally.

There are scalar mesons which are established experimentally, so that one is then tempted to classify them as belonging to an octet of pure $q\bar{q}$ content. This octet however appears to be rather unusual: (i) the $f_0(975)$, assumed to have a certain s-quark content, is lighter than the $a_0(980)$ which is often assumed to have no s-

TABLE II. Main fits of low-energy quantities in the QMC.

Process	QCM	Expt.
$f_\pi = \frac{\Lambda}{\pi} \frac{\sqrt{3} R_P(\mu_\pi^2)}{\sqrt{2 R_{PP}(\mu_\pi^2)}}$	132 MeV	132 MeV
$f_K = \frac{\Lambda}{\pi} \frac{\sqrt{3} R_P(\mu_K^2)}{\sqrt{2 R_{PP}(\mu_K^2)}}$	158 MeV	157 MeV
$g_{\rho\gamma} = \frac{1}{\pi} \frac{R_V(\mu_\rho^2)}{\sqrt{8 R_{VV}(\mu_\rho^2)}}$	0.18	0.20
$g_{\pi\gamma\gamma} = \frac{1}{\Lambda} \frac{R_{PVV}(\mu_\pi^2)}{\pi \sqrt{3 R_{PP}(\mu_\pi^2)}}$	0.26 GeV^{-1}	0.276 GeV^{-1}
$g_{\omega\pi\gamma} = \frac{1}{\Lambda} \frac{\sqrt{6} R_{PVV}(\mu_\omega^2)}{\sqrt{R_{PP}(\mu_\pi^2) R_{VV}(\mu_\omega^2)}}$	2.09 GeV^{-1}	2.54 GeV^{-1}
$g_{\rho\pi\pi} = \frac{\pi \sqrt{8} R_{VPP}(\mu_\rho^2)}{R_{PP}(\mu_\pi^2) \sqrt{R_{VV}(\mu_\rho^2)}}$	6.0	6.1

quark contribution (note however that there is a model in which both of these mesons are assumed to be the molecular states of $K\bar{K}$ [25]), and (ii) the $f_0(1400)$, previously called ε (1300), appears to be a little too heavy to be classified as in the same lowest octet as the f_0 and a_0 discussed above. Thus it is often assumed that this $f_0(1400)$ is a scalar with radial excitation. These unusual features suggest that, in fact, scalar mesons should have a more complicated structure than that arising from the simple quark current ($\propto \bar{q}q$). There are suggestions that they may be $qq\bar{q}\bar{q}$ states [26], or of hybrid glueball nature [27], but it is very difficult to construct a realistic model with a concrete prediction based upon such pictures (for example, there are quite a lot of four-quark currents if one allows the color-nonsinglet contributions).

In the previous QCM approach [20], it was found that with the simple scalar quark current given above, the matrix element describing the decay $S \to \pi\pi$ goes to zero when the scalar meson mass is equal to 1070 MeV. It is thus impossible to describe the observed decay $f_0(975) \to \pi\pi$. To remedy this trouble and to model the complicated inner structure of scalar mesons in a simplest possible manner, an auxiliary contribution with derivative was included in the scalar quark current:

$$\Gamma_{(M=S)} = I - iH \overleftrightarrow{\partial} /\Lambda. \tag{10}$$

Together with parameter H in this current, the angle for the singlet-octet mixing δ_S ($\delta_S \equiv \theta_S - \theta_I$, $\theta_I \equiv$ ideal mixing angle) for f_0 and ε, and the mass m_ε were taken as adjustable parameters. In Ref. [20] there are some errors in the equations used to find the best values for those parameters. We have corrected them and made a refit in the present work.

There are three quantities used for this objective. Two of them are the $\pi\pi \to \pi\pi$ and $\gamma\pi^0 \to \gamma\pi^0$ amplitudes in the chiral (zero energy, zero mass) limit for which they must vanish: the Adler consistency condition [23] as illustrated in Fig. 2. The corresponding equations read

$$P_1 \equiv B_0 - 2\Lambda^2(A_0 - 4HB_1)^2[\cos^2\delta_S\, h_\varepsilon D_\varepsilon(0) + \sin^2\delta_S\, h_{f_0} D_{f_0}(0)] = 0, \tag{11}$$

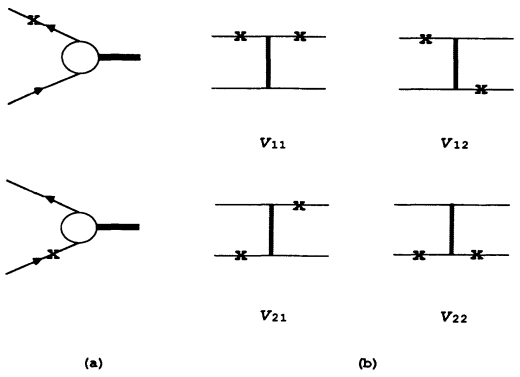

FIG. 2. Consistency conditions used to constrain the scalar-meson parameters.

$$P_2 \equiv b(0) - 2\Lambda^2 a(0)(A_0 - 4HB_1) \times \left(\cos^2\delta_S\, h_\varepsilon D_\varepsilon(0) + \sin^2\delta_S\, h_{f_0} D_{f_0}(0) - \frac{\sqrt{2}}{5}\sin\delta_S\cos\delta_S[h_\varepsilon D_\varepsilon(0) - h_{f_0} D_{f_0}(0)]\right) = 0, \tag{12}$$

where

$$D_M(p^2) = \frac{1}{h_M \tilde{\Pi}_M(p^2) + m_M^2 - p^2}, \tag{13}$$

with $\tilde{\Pi}_M(p^2)$ being the renormalized meson-mass operator in a single-quark loop approximation which is an entire function in the QCM, and

$$A_0 \equiv \int_0^\infty du\, a(u) = 1.09, \quad A_1 \equiv \int_0^\infty du\, ua(u) = 0.45,$$

$$B_0 \equiv \int_0^\infty du\, b(u) = 2.26, \quad B_1 \equiv \int_0^\infty du\, ub(u) = 1.45.$$

In order to obtain these conditions, one calculates the amplitudes which are quite similar to those for obtaining the electromagnetic polarizabilities of pseudoscalar mesons described in the next section. Here we have only to calculate what are called the box and the scalar meson exchange contributions in the limit where the pion mass vanishes. As it has turned out, the scalar meson contributions in Eqs. (11) and (12) are rather insensitive to the change in δ_S, which may be understood since the masses of f_0 and ε (hence the values of their coupling constants) cannot be very different. However, these contributions are quite sensitive to the change in H, and moderately so to the change in m_ε.

The third quantity is the pionic decay width of the $f_0(975)$, for which $\Gamma(f_0 \to \pi\pi) = 24 \pm 5$ MeV experimentally. The scalar-meson pionic decay width [see Fig. 3(a)] is written as

$$\Gamma(S \to \pi\pi) = \frac{3}{32\pi}\sqrt{1 - \frac{4m_\pi^2}{m_S^2}}\frac{G_{S\pi\pi}^2}{m_S},$$

with

$$G_{S\pi\pi} = \Lambda\pi h_\pi^2 C_{S\pi\pi}\sqrt{\frac{h_S}{6}} F_{SPP}(\mu_S^2, 0, 0), \tag{14}$$

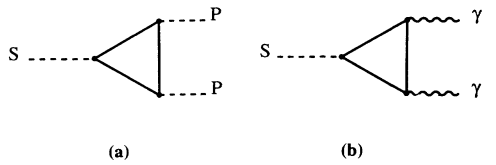

FIG. 3. Diagrams describing scalar-meson decays (a) $S \to PP$, (b) $S \to \gamma\gamma$.

where the function $F_{SPP}(x,y,z)$ and the SU(3) factors $C_{S\pi\pi}$ are given in Appendix C. In the above equation $\mu_S \equiv m_S/\Lambda$. *Note that this definition applies to other mesons throughout the rest of this article.* It is then clear that $\Gamma[f_0(975) \to \pi\pi]$ is proportional to $\sin^2\delta_S$ and, thus, sensitive to δ_S. It is also sensitive to the change in H, but does not depend on m_ε.

In our present study, the best fit to the consistency conditions and the decay width for $f_0 \to \pi\pi$ has been achieved with

$$H = -0.15, \quad \sin\delta_S = 0.3, \quad m_\varepsilon = 1040 \text{ MeV}. \tag{15}$$

The fitting results are [recall Eqs. (11), (12)]

$$P_1 = -0.1, \qquad P_2 = -0.33,$$

and

$$\Gamma(f_0 \to \pi\pi) = 20 \text{ MeV}.$$

The calculated decay width is in good agreement with the experimental value quoted above.

With these parameters determined above, we have calculated (i) the isospin zero and two $\pi\pi$ scattering lengths and (ii) other decay widths of scalar mesons. By neglecting the pion mass in the quark loop integrals, we find the s-wave $\pi\pi$ scattering lengths

$$a_0^0 = 0.11, \quad a_0^2 = -0.05 \quad (\text{units } m_\pi = 1).$$

Experimentally, they are [28]

$$a_0^0 = 0.23 \pm 0.05, \quad a_0^2 = -0.05 \pm 0.03$$

(units $m_\pi = 1$).

The model predicts the decay width

$$\Gamma(\varepsilon \to \pi\pi) = 180 \text{ MeV}.$$

This is consistent with that of $f_0(1400)$. However, our ε mass is not really close to 1400 MeV. There is another scalar meson $f_0(1260)$ identified in the phase shift analysis of the $K_S^0 K_S^0$ system, but the details of its properties are not well known [14].

Further, we have calculated the radiative decay of scalar mesons. This decay is defined by the diagram Fig. 3(b). The matrix element corresponding to this diagram reads

$$M_{S\gamma\gamma} = e^2 G_{S\gamma\gamma}\epsilon_1^\mu \epsilon_2^\nu (g^{\mu\nu} q_1 q_2 - q_1^\nu q_2^\mu), \tag{16}$$

where $\epsilon_1^\mu, \epsilon_2^\nu$ are photon polarizations and

$$G_{S\gamma\gamma} = \frac{1}{\Lambda}\frac{\sqrt{6h_S}}{2\pi} F_{S\gamma\gamma}(\mu_S^2) C_{S\gamma\gamma}.$$

The function $F_{S\gamma\gamma}(\mu_S^2)$ and the SU(3) factors $C_{S\gamma\gamma}$ are given in Appendix C. Finally, the decay width is

$$\Gamma(S \to \gamma\gamma) = \frac{\pi}{4}\alpha^2 m_S^3 G_{S\gamma\gamma}^2.$$

The numerical results are shown in Table III.

It should be remarked here that to determine the scalar-meson parameters H, δ_s, and m_ε, it is possible to use the $\pi\pi$ scattering phase shift and/or the corresponding scattering lengths. This has actually been done [29] and the result indicates that the ε mass should be around 1000 MeV. On the other hand, the calculated phase shift appears rather insensitive to the value of H. So it is important to retain one of the equations from the consistency condition: Eqs. (11) and (12).

Concluding this section, we reiterate that our model for scalar mesons is a rather simple-minded one, but the objective of this article is not to explain the bulk of the scalar-meson properties correctly: this itself would be a formidable task in quark models. Our scalar propagators do not contain the contribution from the decay widths. This treatment is in line with the zeroth order in the $1/N_C$ expansion upon which our present model is based, and will be touched upon in the next section (see also Ref. [19]): the propagator whose mass operator properly includes the meson decay width effect can only be obtained by including the terms of at least $O(1/N_C)$ in this expansion. Thus a naive estimate is that our treatment in the scalar mesons sector is correct within $\sim 30\%$. However, we note that (i) we have constrained our three parameters by two self-consistency conditions, (ii) we have obtained a reasonable prediction for the available scalar-meson decay widths, and (iii) the same treatment of the scalar mesons has given an adequate description of the π-π phase shifts [29]. Also, the consistency conditions are for the soft pion, and we shall deal with the zero energy Compton amplitude needed to extract the polarizabilities. For these the meson widths may not play an essential role. This gives us some confidence that presumably for the present purpose our model is relevant and its effective accuracy to be less than 30%.

III. COMPTON AMPLITUDE AND THE POLARIZABILITIES

A. Preliminaries

First, as pointed out, for example, by Friar [2], it is important to keep in mind that while physical amplitudes describing electromagnetic processes are independent of the system of units adopted, this does not apply to the electromagnetic polarizabilities. Theorists prefer the

TABLE III. Decay widths of scalar and axial-vector mesons.

Mode	QCM	Expt. (Ref.14)
$f_0 \to \pi\pi$	20 MeV	24 ± 5 MeV
$\varepsilon \to \pi\pi$	180 MeV	140–360 MeV for $f_0(1400)$ meson
$f_0 \to \gamma\gamma$	2.4 keV	
$a_0 \to \gamma\gamma$	2.4 keV	
$\varepsilon \to \gamma\gamma$	6.4 keV	
$a_1 \to \pi\gamma$	300 keV	640 ± 246 keV

Heaviside system in which (in natural units: $c = \hbar = 1$) $e^2/4\pi = 1/137 \equiv \alpha$, where e is the unit charge. On the other hand, in Gaussian (cgs) units, liked by experimentalists, $e^2 = \alpha$. Thus the numerical value of the electric (magnetic) polarizability in the Heaviside system is 4π that in the Gaussian system. In what follows, our calculation relies upon the Heaviside system, but *the obtained polarizabilities will be presented in Gaussian units*, in order to conform to tradition.

Second, for the sake of clarity and in order to facilitate the comparison with other works, we shall outline how one obtains the electromagnetic polarizabilities of pseudoscalar mesons from the Compton amplitude. See, for example, Feinberg and Sucher [30] for a somewhat different approach to this point.

Let us consider low-energy photon scattering by a spinless scatterer with unit charge e and mass m. We characterize the incoming (outgoing) photon with energy ω (ω'), momentum $\mathbf{k}$ ($\mathbf{k}'$), and polarization $\boldsymbol{\epsilon}$ ($\boldsymbol{\epsilon}'$). Then, the corresponding amplitude reads [31, 32], in Gaussian units,

$$F_{\rm NR} = -\boldsymbol{\epsilon}\cdot\boldsymbol{\epsilon}'\frac{\alpha}{m} + \boldsymbol{\epsilon}\cdot\boldsymbol{\epsilon}'\,\omega\omega'\alpha_P + (\boldsymbol{\epsilon}\times\mathbf{k})\cdot(\boldsymbol{\epsilon}'\times\mathbf{k}')\beta_P, \tag{17}$$

where α_P and β_P are the electric and magnetic polarizabilities, respectively. The first term in the amplitude is due to the Thomson scattering which is zero for a neutral scatterer, while the remainder is essentially the Rayleigh scattering which contains the information on the polarizabilities. We note that what is called the form-factor contribution is included in our definition of α_P and β_P [4, 11, 33].

Next, we write the general form of the invariant amplitude for the photon scattering by a pseudoscalar meson of unit charge e, and try to extract the expressions for the polarizabilities. This may be done by taking a very-low-energy limit of the amplitude, then comparing it with the nonrelativistic form given above. We adopt the following notation throughout the rest of this article: p_1, p_2 are the initial and final meson momenta, q_1, q_2 the initial and final photon momenta, ϵ_1, ϵ_2 the initial and final photon polarizations, and $s = (p_1+q_1)^2 = (p_2+q_2)^2$, $t = (p_1 - p_2)^2 = (q_1 - q_2)^2$. On mass shell we have

$$p_1^2 = p_2^2 = m_P^2, \quad q_1^2 = q_2^2 = 0, \quad \epsilon_1\cdot q_1 = \epsilon_2\cdot q_2 = 0.$$

We adopt the normalization convention found in Itzykson and Zuber [34] and express the (elastic) Compton scattering amplitude F_C in terms of the corresponding invariant amplitude M:

$$F_C = \frac{M}{8\pi\sqrt{s}}, \quad M = \epsilon_{1\,\mu}M^{\mu\nu}\epsilon_{2\,\nu}. \tag{18}$$

Then $M^{\mu\nu}$ may be decomposed as

$$M^{\mu\nu} = M^{\mu\nu}_{\rm point} + M^{\mu\nu}_{\rm str}, \tag{19}$$

where the first term is due to scattering from a (structureless) point charge (see Fig. 4), and the second term arises from the inner structure of the meson (including the effect of coupling to other mesons in the intermediate states). Each of these contributions may be written as

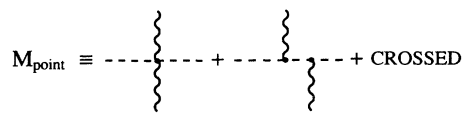

FIG. 4. Compton scattering by a point charge corresponding to $M^{\mu\nu}_{\rm point}$ in the text.

$$M^{\mu\nu}_{\rm point} = 2e^2\left(g^{\mu\nu} + \frac{1}{-p_1\cdot q_1}p_1^\mu p_2^\nu + \frac{1}{p_2\cdot q_1}p_2^\mu p_1^\nu\right), \tag{20}$$

and

$$M^{\mu\nu}_{\rm str} \equiv 4\pi[f_1(s,t)\tilde{T}_1^{\mu\nu} + f_2(s,t)\tilde{T}_2^{\mu\nu}], \tag{21}$$

where the reason for the extra 4π factor in the above definition will become clear later. In the last equation above, the two gauge-invariant Lorentz tensors take the forms

$$\tilde{T}_1^{\mu\nu} = q_2^\mu P_2^\nu(q_1\cdot P_1) + P_1^\mu q_1^\nu(P_2\cdot q_2) - P_1^\mu P_2^\nu(q_1\cdot q_2) - g^{\mu\nu}(P_1\cdot q_1)(P_2\cdot q_2), \tag{22}$$

and

$$\tilde{T}_2^{\mu\nu} = g^{\mu\nu}(q_1\cdot q_2) - q_2^\mu q_1^\nu, \tag{23}$$

where $P_i \equiv p_i/m_P$. Note that the first of these tensors is somewhat different from the often used $T_i^{\mu\nu}$ [30]: the relation between them is

$$\tilde{T}_1^{\mu\nu} = -\frac{1}{4}T_1^{\mu\nu} - \frac{1}{4m_P^2}T_2^{\mu\nu}(4q_1\cdot p_1 - q_1\cdot q_2), \tag{24}$$

and

$$\tilde{T}_2^{\mu\nu} = T_2^{\mu\nu}. \tag{25}$$

Now we take a very-low-energy limit of our amplitude F_C to compare with $F_{\rm NR}$ of Eq. (17). We adopt the transverse gauge in which the time component of the polarization vector vanishes, so $\epsilon_i = (0, \boldsymbol{\epsilon}_i)$. One then finds

$$\epsilon_{1\,\mu}\tilde{T}_1^{\mu\nu}\epsilon_{2\,\nu} \sim \boldsymbol{\epsilon}_1\cdot\boldsymbol{\epsilon}_2\, q_{10}q_{20}, \tag{26}$$

and

$$\epsilon_{1\,\mu}\tilde{T}_2^{\mu\nu}\epsilon_{2\,\nu} \sim -\boldsymbol{\epsilon}_1\cdot\boldsymbol{\epsilon}_2\, q_{10}q_{20} + (\boldsymbol{\epsilon}_1\times\mathbf{q}_1)\cdot(\boldsymbol{\epsilon}_2\times\mathbf{q}_2). \tag{27}$$

In a similar manner one finds that in the low-energy limit

$$\frac{\epsilon_{1\,\mu}M^{\mu\nu}_{\rm point}\epsilon_{2\,\nu}}{8\pi\sqrt{s}} \longrightarrow -\frac{\boldsymbol{\epsilon}_1\cdot\boldsymbol{\epsilon}_2\, e^2}{4\pi m_P}. \tag{28}$$

Then one obtains (in the Heaviside units) for $s \to m_P^2$ and $t \to 0$

$$F_C \to -\frac{\boldsymbol{\epsilon}_1\cdot\boldsymbol{\epsilon}_2\alpha}{m_P} + \frac{\boldsymbol{\epsilon}_1\cdot\boldsymbol{\epsilon}_2\, q_{10}q_{20}[f_1(m_P^2,0) - f_2(m_P^2,0)]}{2m_P} + \frac{(\boldsymbol{\epsilon}_1\times\mathbf{q}_1)\cdot(\boldsymbol{\epsilon}_2\times\boldsymbol{\epsilon}_2)f_2(m_P^2,0)}{2m_P}, \tag{29}$$

so by comparing this with Eq. (17), the following identifications result:

$$\alpha_P = \frac{f_1(m_p^2,0) - f_2(m_P^2,0)}{2m_P}, \quad \beta_P = \frac{f_2(m_P^2,0)}{2m_P}. \tag{30}$$

We note that because of the extra factor 4π in Eq. (21), the values of the electromagnetic polarizabilities, calculated in the above expression using Heaviside units, are given in *Gaussian units*. From the last equation, one obtains

$$\alpha_P + \beta_P = \frac{f_1(m_P^2,0)}{2m_P}. \tag{31}$$

As mentioned in our Introduction, this combination of polarizabilities vanishes in the chiral limit, so one finds

$$f_1(0,0) = 0, \tag{32}$$

for pseudoscalar-octet mesons.

B. Calculation of the Compton amplitude and polarizabilities

The Compton scattering amplitude for a pseudoscalar meson in our QCM obtains contributions from the following processes (or diagrams): (1) the photon scattering by a point charge (Fig. 4), (2) diagrams which involve only one quark loop (either △, ○, or □ shape, see Fig. 5) and pseudoscalar meson lines, (3) the t-channel scalar meson exchange [Fig. 6(a)], (4) the s- and u-channel vector- and axial-vector meson exchanges [Figs. 6(b) and (7)]. These contributions may be regarded as the leading- (or the zeroth-) order terms in the $1/N_C$ expansion where N_C (= 3) is the number of colors, and correspond to those from the tree approximation in effective Lagrangian approaches such as the linear and nonlinear σ models. However, the presence of quark loops in QCM diagrams introduces nontrivial momentum dependences which, of course, do not exist in the effective Lagrangian scheme with only meson degrees of freedom.

In the present approach, meson and baryon loop contributions illustrated in Fig. 8 enter as $O(1/N_C)$, so their effects are expected to be at most $\sim 1/3$ of what we are calculating. In principle, we could go up to this order. However, for consistency basic meson and baryon quantities must also be recalculated up to $O(1/N_C)$: for example, the compositeness condition, Eq. (2) must be satisfied to this order. So we shall stay at the level of the leading order here. See discussions on this subject in Sec. IV.

Before presenting the resultant amplitude, it is worth emphasizing that since our confinement function guarantees the ultraviolet convergence of the loop integration, no regularization is needed, with the consequence that electromagnetic gauge invariance is manifest at any stage of the calculation.

Let us give the contributions to the Compton scattering amplitude from separate diagrams. Some details of the calculation may be found in Appendix C. The expressions given below are for photon scattering near threshold.

(1) *Scattering by a point charge* [Figs. 4 and 5(c)]
This arises entirely from the minimal substitution

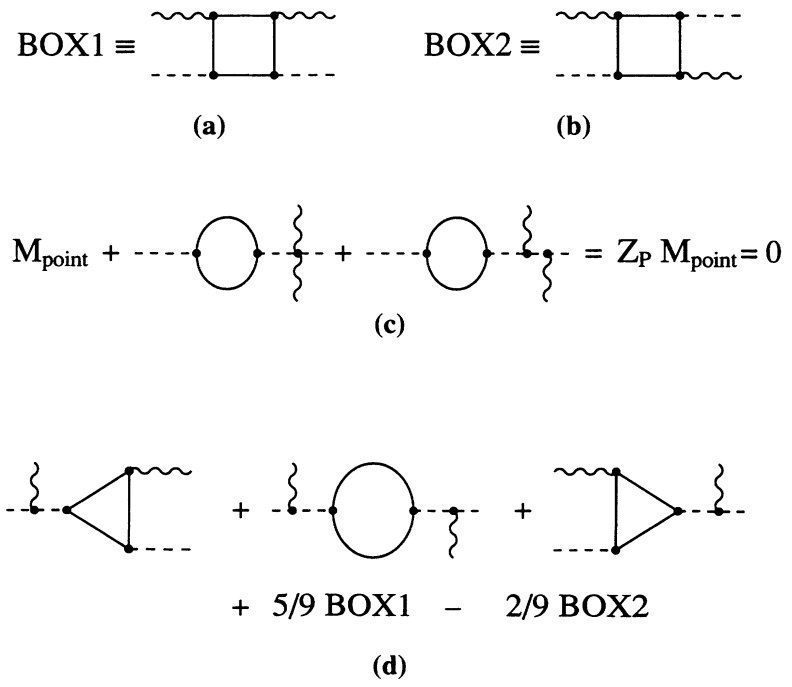

FIG. 5. Triangle, bubble, and box (TBB) contributions to the Compton scattering of pseudoscalar mesons: (a), (b) box diagrams; (c) the consequence of the compositeness condition; (d) contribution to charged mesons. Crossed contributions are implicit.

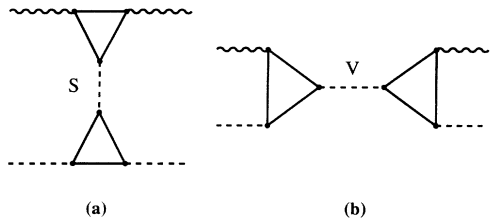

FIG. 6. (a) Scalar- and (b) vector-meson contributions to the Compton scattering of pseudoscalar mesons. Crossed contributions are implicit.

$$\partial_\mu \longrightarrow \partial_\mu - ieA_\mu$$

in the free meson Lagrangian and, of course, vanishes for neutral mesons. The result is $M^{\mu\nu}_{\rm point}$ of Eq. (20). However, the composite nature of our pseudoscalar mesons manifests itself as an additional contribution to this term from the self-energy bubble in the external meson line evaluated on mass shell [Fig. 5(c)]. Because of the compositeness condition, Eq. (2), the sum of all these contributions can be shown to vanish.

(2) *Triangle (form factor), self-energy bubble, and box diagrams: TBB* [Fig. 5(d)]

These contributions arise from single-quark loops forming the pion (kaon) electromagnetic form factor, pion (kaon) self-energy bubble, and the box diagrams. The box diagram has two topologically distinct contributions as shown in Figs. 5(a) and 5(b). We call them TBB in the following. They collectively respect gauge invariance for charged mesons, but not separately. For neutral mesons only the box diagrams Figs. 5(a) and 5(b) contribute.

(a) Neutral mesons:

$$M^{\mu\nu}_{{\rm TBB}\,\pi^0} = \frac{e^2 h_\pi}{\Lambda^2}[\mu_\pi^2 W_1^0(\mu_\pi^2)\tilde{T}_1^{\mu\nu} + W_2^0(\mu_\pi^2)\tilde{T}_2^{\mu\nu}], \tag{33}$$

and

$$M^{\mu\nu}_{{\rm TBB}\,K^0} = \frac{2e^2 h_K}{5\Lambda^2}[\mu_K^2 W_1^0(\mu_K^2)\tilde{T}_1^{\mu\nu} + W_2^0(\mu_K^2)\tilde{T}_2^{\mu\nu}], \tag{34}$$

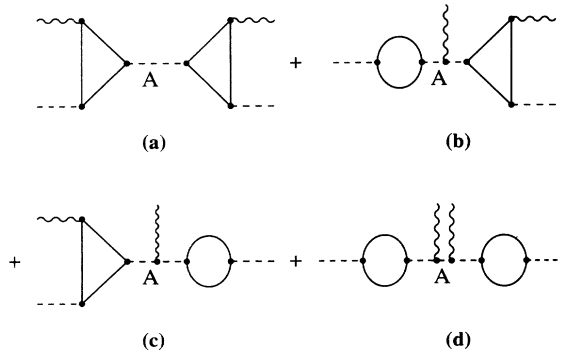

FIG. 7. Axial-vector meson contributions to the Compton scattering of pseudoscalar mesons. Crossed contributions are implicit.

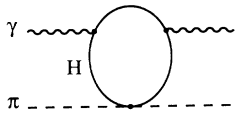

FIG. 8. Typical one-hadron-loop contribution to the $\gamma\pi$ Compton amplitude. H is a hadron, either a meson or baryon.

where, as defined in the preceding section, $\mu_P \equiv m_P/\Lambda$.

(b) Charged mesons. For charged mesons all the diagrams in Fig. 5(d) contribute:

$$M^{\mu\nu}_{\rm TBB} = M^{\mu\nu}_{\rm point} + M^{\mu\nu}_{\rm +SD}, \tag{35}$$

with the inner structure-dependent term being

$$M^{\mu\nu}_{\rm +SD} = \frac{e^2 h_P}{\Lambda^2}[\mu_P^2 W_1^+(\mu_P^2)\tilde{T}_1^{\mu\nu} + W_2^+(\mu_P^2)\tilde{T}_2^{\mu\nu}]. \tag{36}$$

The functions $W_i^{0,+}(x)$ are given in Appendix C. It is amusing to find that the point charge contribution, once canceled by the compositeness condition, is perfectly restored here. Note that it, of course, does not contribute to the polarizabilities.

(3) *Scalar mesons (S) in t-channel exchange* [Fig. 6(a)]

The contribution to the invariant amplitude reads

$$M_S^{\mu\nu} = \tilde{T}_2^{\mu\nu}\frac{-e^2 h_P}{2\Lambda^2} C_{SPP} F_{SPP}(0,\mu_P^2,\mu_P^2) \times C_{S\gamma\gamma} F_{S\gamma\gamma}(0) h_S/\mu_S^2. \tag{37}$$

The structure functions F_S's and the SU(3) factors C_S's are given in Appendix C.

(4) *Axial-vector and vector-meson exchanges in the s and t channels* [Figs. 6(b) and (7)]

(a) Axial-vector mesons (A). The axial-vector mesons contribute only to the Compton scattering of charged particles. The net contribution is

$$M_A^{\mu\nu} = \tilde{T}_1^{\mu\nu}\frac{e^2 h_P}{\Lambda^2}\mu_P^2 F_{AP\gamma}^2(\mu_P^2,\mu_P^2,0)\left(\frac{h_A}{\mu_A^2-\mu_P^2}+\frac{h_A}{\mu_A^2}\right). \tag{38}$$

The structure function $F_{AP\gamma}$ is given in Appendix C.

(b) Vector mesons (V). The vector-meson contribution is obtained as

$$M_V^{\mu\nu} = [\tilde{T}_1^{\mu\nu} + \tilde{T}_2^{\mu\nu}]\frac{e^2 h_P}{4\Lambda^2}\mu_P^2 C_{VP\gamma}^2 F_{PVV}^2(\mu_P^2,\mu_P^2,0) \times\left(\frac{h_V}{\mu_V^2-\mu_P^2}+\frac{h_V}{\mu_V^2}\right). \tag{39}$$

The structure function F_{PVV} is given in Appendix C.

From the different pieces contributing to the invariant Compton amplitude presented above, and from Eqs. (21) and (30), we can extract the electromagnetic polarizabilities from each individual contribution: TBB, the exchange of scalar, vector, and axial-vector mesons. They are given in Table IV, in which one finds several interesting points. First, vector meson exchange contributes

only to the magnetic polarizability, whereas axial-vector exchanges give finite contribution only to the electric polarizabilities. Second, these two contributions are of $O(\mu_P^2)$, so they vanish in the zero mass (chiral) limit of the pseudoscalar mesons:

$$\mu_P^2 \longrightarrow 0 \quad (P \equiv \pi \text{ and } K)$$

[note that m_P in the denominator of each separate contribution to the polarizability is not subject to this limiting procedure: its origin is the defining relation, Eq. (30)]. Third, the surviving contributions in this limit are the scalar exchange and a part of TBB which are found to satisfy the well-known relation [recall the discussion in Sec. I, and Eqs. (31) and (32)]

$$\alpha_P + \beta_P \propto f_1(0,0) = 0. \tag{40}$$

Thus, our result explicitly shows that this relation is violated to $O(\mu_P^2)$. This must result from any reasonable model (see, for example [6, 9]).

Any further discussion needs concrete numerical results which will be relegated to the next section.

IV. DISCUSSION AND CONCLUSION

Contributions listed in Table IV are evaluated numerically and are presented in Table V. From the table one

TABLE IV. Analytic expressions for pseudoscalar-meson electromagnetic polarizabilities in the present model.

	TBB	Scalar
α_{π^0}	$\frac{\alpha h_\pi}{2\Lambda^2 m_\pi}[-W_2^{(0)}(\mu_\pi^2) + \mu_\pi^2 W_1^{(0)}(\mu_\pi^2)]$	$\frac{\alpha h_\pi}{9\Lambda^2 m_\pi} F_{SPP}(0,\mu_\pi^2,\mu_\pi^2) F_{S\gamma\gamma}(0) I_S^\pi$
β_{π^0}	$\frac{\alpha h_\pi}{2\Lambda^2 m_\pi} W_2^{(0)}(\mu_\pi^2)$	$-\alpha_{\pi^0}$
α_{π^+}	$\frac{\alpha h_\pi}{2\Lambda^2 m_\pi}[-W_2^{(+)}(\mu_\pi^2) + \mu_\pi^2 W_1^{(+)}(\mu_\pi^2)]$	α_{π^0}
β_{π^+}	$\frac{\alpha h_\pi}{2\Lambda^2 m_\pi} W_2^{(+)}(\mu_\pi^2)$	$-\alpha_{\pi^0}$
α_{K^0}	$\frac{\alpha h_K}{5\Lambda^2 m_K}[-W_2^{(0)}(\mu_K^2) + \mu_K^2 W_1^{(0)}(\mu_K^2)]$	$\frac{\alpha h_K}{18\Lambda^2 m_K} F_{SPP}(0,\mu_K^2,\mu_K^2) F_{S\gamma\gamma}(0) I_S^{K^0}$
β_{K^0}	$\frac{\alpha h_K}{5\Lambda^2 m_K} W_2^{(0)}(\mu_K^2)$	$-\alpha_{K^0}$
α_{K^+}	$\frac{\alpha h_K}{2\Lambda^2 m_K}[-W_2^{(+)}(\mu_K^2) + \mu_K^2 W_1^{(+)}(\mu_K^2)]$	$\frac{\alpha h_K}{18\Lambda^2 m_K} F_{SPP}(0,\mu_K^2,\mu_K^2) F_{S\gamma\gamma}(0) I_S^{K^+}$
β_{K^+}	$\frac{\alpha h_K}{2\Lambda^2 m_K} W_2^{(+)}(\mu_K^2)$	$-\alpha_{K^+}$
	Vector	Axial vector
α_{π^0}	0	0
β_{π^0}	$\frac{10\alpha h_\pi}{9\Lambda^2 m_\pi} \mu_\pi^2 F_{PVV}^2(\mu_\pi^2,\mu_\pi^2,0) I_V^\pi$	0
α_{π^+}	0	$\frac{\alpha h_\pi}{\Lambda^2 m_\pi} \mu_\pi^2 F_{AP\gamma}^2(\mu_\pi^2,\mu_\pi^2,0) I_A^\pi$
β_{π^+}	$\frac{1}{10}\beta_{\pi^0}$	0
α_{K^0}	0	0
β_{K^0}	$\frac{4\alpha h_K}{9\Lambda^2 m_K} \mu_K^2 F_{PVV}^2(\mu_K^2,\mu_K^2,0) I_V^K$	0
α_{K^+}	0	$\frac{\alpha h_K}{\Lambda^2 m_K} \mu_K^2 F_{AP\gamma}^2(\mu_K^2,\mu_K^2,0) I_A^K$
β_{K^+}	$\frac{1}{4}\beta_{K^0}$	0

$$I_S^\pi = 5[\cos^2\delta_S h_\epsilon D_\epsilon(0) + \sin^2\delta_S h_{f_0} D_{f_0}(0)]\Lambda^2 - \sqrt{2}\sin\delta_S\cos^2\delta_S[h_\epsilon D_\epsilon(0) - h_{f_0} D_{f_0}(0)]\Lambda^2$$

$$I_S^{K^0} = 3[\cos^2\delta_S h_\epsilon D_\epsilon(0) + \sin^2\delta_S h_{f_0} D_{f_0}(0)]\Lambda^2 + \{2[h_\epsilon D_\epsilon(0) + h_{f_0} D_{f_0}(0)] - 3h_{a_0} D_{a_0}(0)\}\Lambda^2 - 6\sqrt{2}\sin\delta_S\cos^2\delta_S[h_\epsilon D_\epsilon(0) - h_{f_0} D_{f_0}(0)]\Lambda^2$$

$$I_S^{K^+} = 3[\cos^2\delta_S h_\epsilon D_\epsilon(0) + \sin^2\delta_S h_{f_0} D_{f_0}(0)]\Lambda^2 + \{2[h_\epsilon D_\epsilon(0) + h_{f_0} D_{f_0}(0)] + 3h_{a_0} D_{a_0}(0)\}\Lambda^2 - 6\sqrt{2}\sin\delta_S\cos^2\delta_S[h_\epsilon D_\epsilon(0) - h_{f_0} D_{f_0}(0)]\Lambda^2$$

$$I_V^\pi = \tfrac{1}{2}[h_\rho D_\rho(m_\pi^2) + h_\rho D_\rho(0)]\Lambda^2$$
$$I_V^K = \tfrac{1}{2}[h_{K^*} D_{K^*}(m_K^2) + h_{K^*} D_{K^*}(0)]\Lambda^2$$

$$I_A^\pi = \tfrac{1}{2}[h_a D_a(m_\pi^2) + h_a D_a(0)]\Lambda^2$$
$$I_A^K = \tfrac{1}{2}[h_{K_1} D_{K_1}(m_K^2) + h_{K_1} D_{K_1}(0)]\Lambda^2$$

TABLE V. Numerical results for polarizability in the Gaussian system. The unit is 10^{-43} cm^3.

	TBB	S	V	A	Total
α_{π^0}	−3.013	3.755	0	0	0.74
β_{π^0}	2.951	−3.755	0.506	0	−0.30
α_{π^+}	−0.140	3.755	0	0.0187	3.63
β_{π^+}	0.295	−3.755	0.051	0	−3.41
α_{K^0}	−0.283	0.610	0	0	0.33
β_{K^0}	0.162	−0.610	0.741	0	−0.29
α_{K^+}	0.678	1.543	0	0.061	2.28
β_{K^+}	0.045	−1.543	0.185	0	−1.31

immediately observes certain trends. The first is that for both pions and kaons, the axial-vector contribution is almost negligible and thus may safely be omitted. The vector-meson contribution also has relatively small magnitude, particularly for the pion polarizability. Next, one sees that the major effect (in magnitude) comes from the scalar exchanges. For neutral mesons this is largely compensated by the TBB diagrams due to the consistency condition (recall Sec. II), which is however not quite obvious for the case of K^0. In any event, it is this compensation which makes the role of the vector exchange visible in the magnetic polarizability of the neutrals. Lastly, the TBB contribution to the kaon polarizability is about an order of magnitude smaller than that for the pion. This arises primarily from the ratio of the coefficients in the TBB contribution:

$$\frac{\alpha}{x\Lambda^2 m_P} \quad (P=\pi,K, \quad x=2,5), \tag{41}$$

as in Table IV. However, there is a very interesting exception to this tendency: the TBB contribution to K^+ is about five times larger than that for π^+ and with opposite sign. The origin of this may be traced to the $W^{(+)}$ function for α_P^+ (see Table IV):

$$W^{(+)}(\mu_P^2) \equiv W_2^{(+)}(\mu_P^2) + \mu_P^2 W_1^{(+)}(\mu_P^2), \tag{42}$$

which arises from the quark loop effect. The μ_P^2 dependence of this function is plotted in Fig. 9. Clearly, for small μ_P^2 ($\mu_\pi^2 = 0.09$) the first term is dominant and the whole expression stays small and negative. But for large μ_P^2 (as in the case of α_{K^+} : $\mu_K^2 = 1.2$) the second term grows rapidly and becomes dominant. Also plotted in Fig. 9 is the corresponding function $W^{(0)}$ for neutral mesons. This is rather flat as a function of μ_P^2, so unlike for charged mesons nothing peculiar happens for $\alpha_{P^{(0)}}$.

For the contribution to the π and K polarizabilities from the scalar-meson exchanges, the ratio

$$\left(\frac{\alpha_K}{\alpha_\pi}\right)_{\text{scalar}} \simeq \frac{m_\pi}{2m_K} \tag{43}$$

may be expected to hold as for the TBB contribution above (see Table IV). This is roughly so for the neutral mesons, but for the charged mesons the ratio is quite larger. The origin of this enhancement is in the factor $I_S^{K^+}$ in Table IV: suppose that all the scalar mesons become degenerate (in fact this is the exact chiral symmetric limit in the context of our present model, which will be discussed later). Then because of the coherent contribution of ε, f_0, and a_0, this factor becomes twice as large as the corresponding factor I_S^π for the pion, and about two and a half times larger than the factor $I_S^{K^0}$ for the neutral kaon. Actually, taking into account Eq. (43), the relative magnitudes of the scalar-meson contribution in Table V can be understood well. Note that this indicates the smooth variation of $F_{SPP}(0,\mu_P^2,\mu_P^2)$ (Table IV) as a function of μ_P^2, which we have actually confirmed.

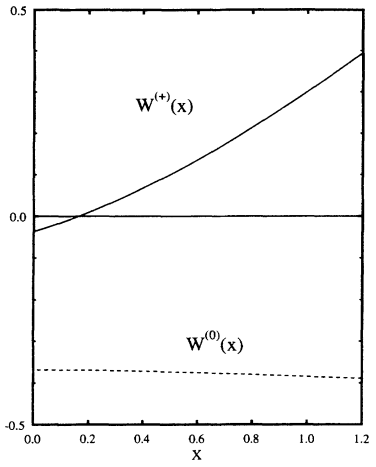

FIG. 9. Functions $W^{(I)}(x) \equiv -W_2^{(I)}(x) + xW_1^{(I)}(x)$ ($I = 0,+$) (see Table IV) appearing in the TBB contribution to the polarizability. Not shown are the minimum $W_{\min}^{(0)} \sim -0.4$ at $x \sim 2.0$ and the maximum $W_{\max}^{(+)} \sim 1.6$ at $x \sim 4.5$.

Summarizing the result in Table V, the total contribution to the charged pion is

$$\alpha_{\pi^+} = 3.6,$$

which is between the LVR's and SVR's. The sum of the electric and magnetic polarizabilities is

$$\alpha_{\pi^+} + \beta_{\pi^+} = 0.22,$$

consistent with 0.39 ± 0.04 from the pion total photoreaction cross section [1, 35]. For the kaon we find

$$\alpha_K^+ = 2.3, \quad \alpha_K^+ + \beta_K^+ = 1.0.$$

Here the effect of chiral symmetry breaking is appreciable as, otherwise, the second quantity would be close to zero while the first one should satisfy

$$\frac{\alpha_K^+}{\alpha_\pi^+} = \frac{m_\pi F_\pi^2}{m_K F_K^2} \sim \frac{1}{5},$$

(see, for example, predictions from chiral models [3, 4, 9]). This rather large charged-kaon polarizability gives us hope that it could be measured without major difficulty (relative to that for the pion) at a future kaon factory.

As for the polarizabilities of the neutral pion and kaon, our result presents rather small values which are basically dictated by the low-energy consistency condition.

Our α_{π^0} is found to be positive as compared with several model results with a negative sign [8,9]. In any event, it appears to be rather difficult to measure the electromagnetic polarizabilities of the neutral mesons if one accepts the result of the existing models (including our present one).

In our present approach the largest model dependence may be found in modeling the scalar mesons which give a major contribution to the polarizabilities. Then how reliable is our prediction here? In this respect we stress that within the context of our model, viz., the leading order in the $1/N_C$ expansion, the parameters in the scalar-meson sector are well controlled by two equations due to the Adler consistency condition, and by the scalar-meson decay widths, and therefore may not vary much. As stated in Sec. II, we cannot change either δ_S or H very much from the present values. A mild shift in m_ϵ may be tolerated. A preliminary numerical test has indicated that the scalar-meson contribution could vary within 10% or so, mostly towards the direction of reducing this contribution. Therefore, our principal conclusion may not change, especially for the charged-kaon electric polarizability. A more reasonable way of determining the scalar-meson parameters may be to use (i) the consistency condition, (ii) the scattering lengths, and (iii) the phase shifts, all in the $\pi\pi$ scattering channel, together with the scalar-meson decay widths. One may then constrain those parameters by χ^2 minimizations. In this case, fit to the phase shifts will principally constrain the ε meson mass. Note that to consistently carry this program out, one needs to go up to $O(1/N_C)$. We shall try to do this in our future study.

In order to understand the consequence of our model somewhat better, we shall analyze the predictions of other (chiral) models (in a somewhat different context there is a comparison of various chiral model predictions [18] which the interested reader is referred to). For this purpose it should be sufficient to discuss only $\alpha_{\pi^\pm}$ and α_{π^0}. Also it may be useful to introduce a physical constant characterizing the size of the polarizabilities: we denote this quantity as κ, defined as one-half the value of what is called the (electromagnetic) form-factor contribution, viz., the finite-size effect, to the polarizability [1, 2, 4, 11]:

$$\kappa \equiv \frac{1}{2}\alpha_\pi^{\mathrm{FF}} = \frac{\alpha\langle r_\pi^2\rangle}{6m_\pi}, \tag{44}$$

Then with the aid of the vector-dominance hypothesis and the Kawarabayashi-Suzuki-Fayyazuddin-Riazuddin (KSFR) relation as in [11], the above expression may be rewritten as

$$\kappa = \frac{2\alpha}{m_\pi(4\pi F_\pi)^2} \ (\simeq 6), \tag{45}$$

where the appearance of a typical chiral expansion parameter $1/(4\pi F_\pi)^2$ is to be noted.

Now we split the total contribution to the electric polarizability into three parts:

$$\alpha(\mathrm{tot}) = \alpha(A) + \alpha(B) + \alpha(C),$$

where A is the tree contribution, B is the contribution from the single-pion loop, and C comes from the single-baryon loops. A typical contribution for B and C is illustrated diagramatically in Fig. 8. Table VI should be useful to see which of these contributions is taken into account in each of the models discussed below as well as its prediction.

Contribution C was included only by Volkov and Pervushin [10] in a nonlinear σ model. The loop structure is similar to that for the quark loop contribution for A as in Fig. 5. They found that for charged pions this occupies more than 90% of the total: $\sim 1.7 g_A^2\kappa/3$ where the factor 1.7 is the effect of including all the octet baryons (according to Ref. [7] this factor should be about 2.1). For the neutral pion this contribution was found to be zero. It is interesting that this result is quite similar to the contribution A found in [7–9]. However, the approach of [10] was shown to give a poor prediction of the pion electromagnetic radius [18]. We thus think that it should not be taken seriously. Yet the treatment of the pion loop is adequate in this reference, so we quote it here and below.

As for the pion loop contribution B, it was considered in a linear σ model by, for example, L'vov [8], and in a nonlinear σ model by Volkov and Pervushin [10]. It was also discussed in the context of CHPT by Donoghue and Holstein [18], and by Holstein [3] based upon the calculation of the $\gamma\gamma \to \pi\pi$ processes [36,37]. Irrespective of the model adopted, this contribution is finite and is found to be negative (or zero) as long as all the participating diagrams are properly included. Thus, unlike in [11], no regularization of the integration is needed.

The results of the above models are summarized in Table VII. The prediction of the linear σ model [8] was obtained by taking the limit $m_\sigma \to \infty$, which is often regarded as the result corresponding to the nonlinear realization of chiral symmetry [23]. For the prediction of Ref. [10], case 1 is the original one in which the coefficient of the direct $\pi\pi$ interaction in the effective Lagrangian is chosen to be 1/3 (the Gürsey choice); it is 1/2 (the Weinberg choice) in case 2 [8, 10]. Since the latter is found to be consistent with the linear σ model and also

TABLE VI. Pion electric polarizability from various models. Tree, pion loop, and baryon loop contributions are indicated by A, B, and C, respectively. The unit is the same as in Table V.

Model	Effect included	$\alpha_{\pi^\pm}$	α_{π^0}
Chiral quark loop Ref. [7]	A	5.8	0
Nonlinear σ model Ref. [10]	BC	5.0	−0.7
Linear σ model Ref. [8]	AB	4.3	−0.7
Superconducting type σ model Ref. [9]	A	5.1	−0.8
Chiral perturbation theory Ref. [18]	A	2.8	0
QCM	A	3.6	0.7

TABLE VII. Pion loop contribution to the pion electric polarizability from several models. The unit is κ [see Eqs. (44) and (45)].

Model	$\alpha_{\pi^\pm}(B)$	$\alpha_{\pi^0}(B)$
Nonlinear σ model (Case 1) Ref. [10]	$-1/18$	$-1/9$
Nonlinear σ model (Case 2) Refs. [8,10]	0	$-1/12$
Linear σ model Ref. [8]	$-1/3$	$-1/12$
Chiral perturbation theory Refs. [3,18,35,36]	0	$-1/12$

with CHPT, we will disregard the former. We then find that all three models give an identical contribution to the neutral pion polarizability. However, for the charged pion only the linear σ model predicts a nonvanishing contribution. We then recall that, as stated in Sec. I, the linear σ model gives an inadequate prediction of the coefficients in the $\mathcal{L}_4$ part of the chiral Lagrangian. So we rely on the results from [10] (case 2) and CHPT, and conclude that the pion loop effect vanishes for the charged pion. A couple of remarks may be adequate here in passing: (i) by inspecting the formulas in [36,37] together with the result of case 2, it appears that the kaon loop gives no contribution to either the charged or neutral pion polarizabilities (because one might interpret the discussion in [18] such that only the combination of the pion and kaon loops gives the vanishing contribution to the charged-pion polarizability), and (ii) the particular choice of gauge in [36] is somewhat confusing for our purpose: it might lead one to find the vanishing pion loop contribution also to the neutral-pion polarizability, which is not correct.

As discussed in Sec. III, a naive expectation would be that the pion loop contribution B could become as much as $O(1/N_c)$ or $\sim 30\%$ of A: the tree contribution to be discussed in the following. So the fact that this loop effect vanishes for the charged pion is quite gratifying for those calculations which include only A [7, 9, 18] and our present one. As for the neutral pion, the tree contribution vanishes in the chiral limit, so the loop correction, even being small (~ -0.5 in our unit) becomes important. From Table V (see also Ref. [9]) this is comparable to the effect of finite (pion) mass correction to this quantity at the tree (TBB) level. In any event the (total) neutral-pion polarizability looks quite small in comparison with the corresponding quantity for the charged pion.

Apart from the nonlinear σ model of Volkov and Pervushin [10] where there is no such piece, the tree effect A is the principal contribution. In the CHPT approach this arises from the $\mathcal{L}_4$ part of the effective Lagrangian; the result is

$$\alpha_\pi(A) = \frac{4\alpha}{m_\pi F_\pi^2}(L_9^r + L_{10}^r)x \qquad (x = 1 \text{ for } \pi_\pm, \ = 0 \text{ for } \pi^0), \quad (46)$$

where L_9^r and L_{10}^r are two of the twelve (renormalized) coefficients in $\mathcal{L}_4$ which are fixed by fit to several low-energy quantities [16]. Within the same approach these coefficients are related to the ratio of the vector and axial-vector form factors in the $\pi \to e\nu\gamma$ amplitude:

$$\gamma \sim \frac{h_A(0)}{h_V(0)} = 32\pi^2(L_9^r + L_{10}^r).$$

In fact, L_{10}^r has been determined from the experimental value of γ. Then

$$\alpha_\pi(A) = \frac{\alpha}{8\pi^2 m_\pi F_\pi^2}\gamma x = \kappa\gamma x \qquad (x = 1 \text{ for } \pi_\pm, \ = 0 \text{ for } \pi^0). \quad (47)$$

As mentioned in Sec. I, this gives the value $\alpha_{\pi^\pm} \sim 2.8$, which we have termed a SVR. An expression identical to Eq. (47) is obtained within the current algebra + PCAC approach [5].

In CHPT the effect of the subhadronic degrees of freedom (as well as the effect from those mesons outside the pseudoscalar octet) is implicit in the coefficients L_i (or in γ). Calculations exploiting the chiral quark loop model [7], linear σ models with an explicit coupling to quarks [8, 9], and our QCM all have tried to obtain the tree contribution from a more microscopic point of view. To simplify our discussion, let us take the chiral limit where there is no contribution from the s- and u-channel exchanges of vector and axial-vector mesons (recall our discussion towards the end of Sec. III). Then the contents of the tree contribution in those models are the quark loops (which we have termed as TBB in the preceding section), and the t-channel scalar exchanges: the latter may be considered as equivalent to the σ exchange in the linear σ model of [8], or to the triangular loop created by the direct pion-quark point interaction in the chiral quark loop model [7]. The pion electric polarizability may then be written as [7–9]

$$\alpha_{\pi^0}(A) = -L + S, \quad (48)$$

and

$$\alpha_{\pi^\pm}(A) = \frac{-1}{10}L + S, \quad (49)$$

where L and S are the quark loop and scalar exchange contributions, respectively. In the chiral limit, the tree-level contribution to the neutral-pion polarizability vanishes, so that $L = S$, and

$$\alpha_{\pi^\pm}(A) = \frac{9}{10}L = \frac{\alpha}{8\pi^2 m_\pi F_\pi^2} = \kappa. \quad (50)$$

The difference between this and the CHPT prediction is just the factor γ [see Eq. (47)], which is around 0.5 experimentally [14]. Apparently, even after applying nonzero-pion-mass corrections, the prediction of [7–9] still stays about a factor of 1.5–2.0 larger than that of [5, 18].

In order to understand the origin of the difference between the model predictions leading to LVR's and SVR's (recall Sec. I), we take the exact chiral limit in the context

of our QCM. Here again the surviving contributions are TBB and the scalar exchanges. Furthermore, the scalar mesons become degenerate [9],

$$m_\epsilon = m_{f_0} = m_{a_0} \equiv m_S,$$

and their coupling strengths become identical, too. This yields

$$\alpha_{\pi^0} = \frac{5\alpha h_\pi}{54\Lambda^2 m_\pi}\left(-b(0) + 2a(0)[A_0 - 4HB_1]\frac{h_S}{\mu_S^2}\right), \tag{51}$$

$$\alpha_{K^0} = \frac{\alpha h_K}{27\Lambda^2 m_K}\left(-b(0) + 2a(0)(A_0 - 4HB_1)\frac{h_S}{\mu_S^2}\right), \tag{52}$$

and

$$\alpha_{P+} = \frac{5\alpha h_P}{54\Lambda^2 m_P}\left(-\frac{1}{10}b(0) + 2a(0)(A_0 - 4HB_1)\frac{h_S}{\mu_S^2}\right), \tag{53}$$

which show a basic structure identical to that in Eqs. (48) and (49).

Then, from the fact that the neutral-pion polarizability vanishes, we also find the vanishing of the neutral-kaon polarizability. Furthermore, we get expressions for the charged-meson polarizabilities which are completely free from the scalar-meson parameters:

$$\alpha_{\pi+} = \frac{\alpha h_\pi b(0)}{12\Lambda^2 m_\pi}, \qquad \alpha_{K+} = \frac{m_\pi}{m_K}\frac{h_K}{h_\pi}\alpha_{\pi+}. \tag{54}$$

In the zero-mass limit for the pion and kaon, one finds

$$h_P = \frac{2}{B_0} = \frac{N_c g_P^2}{(2\pi)^2}, \quad F_P = \frac{\sqrt{2}\Lambda A_0}{g_P B_0}, \tag{55}$$

which may be obtained from the compositeness condition [Eq. (2)], and the expression for the meson decay constant in Table II, both of which require $R_P(\mu_P^2)$ and $R_{PP}(\mu_P^2)$ listed in Appendix B, with $\mu_p^2 \to 0$. Then, Eq. (54) becomes

$$\alpha_{P\pm} = \frac{N_c\alpha}{3\times 8\pi^2 m_P F_P^2} y \ \ (= \kappa y \ \text{ for } P = \pi), \tag{56}$$

with

$$y = b(0)\left(\frac{A_0}{B_0}\right)^2. \tag{57}$$

Adopting the values of these constants found in Sec. II, we find $y \sim 0.47$. So in the exact chiral limit we obtain

$$\alpha_{\pi+} = 2.8\times 10^{-43}\ \text{cm}^3, \ \alpha_{K+} = 0.8\times 10^{-43}\ \text{cm}^3,$$

which is just the prediction of the SVR [5, 18].

It is important here to point out the following fact: unlike in CHPT [Eq. (47)] and in the current algebra + PCAC approach [5], y in Eq. (57) and γ in the QCM are apparently not related at the present stage. That is, within the QCM this latter quantity is found to be $\gamma = 0.78$ [19], which is larger than the world average value of 0.46 ± 0.02 [14] (remember, however, that this average contains a recent measurement [38] $\gamma = 0.7 \pm 0.5$). It has been known that this is rather a controversial quantity from the point of view of model predictions (various models have given predictions for γ between zero and one) [39–42]. Thus it is likely that the QCM treatment of this quantity has to be improved. This is what we will pursue in the near future.

From what we have found above within our QCM approach, the following observation emerges: when no confinement is imposed, the tree contribution gives a large value of $\alpha_{\pi\pm}$, as in chiral quark loop and linear σ models. Once quark confinement is implemented, this value is reduced and in the strict chiral limit it virtually agrees with the small value from CHPT.

Now we summarize our results.

(1) For the charged pion, we find a small electric polarizability (~ 2.8), in agreement with the CHPT result when we take the limit of the vanishing pion mass (the chiral limit). Within our QCM we attribute this small value to the effect of quark confinement. Once the finite-pion-mass correction is included, together with the SU(3)-breaking effect in the scalar-meson sector, we get

$$\alpha_{\pi\pm} \simeq 3.6, \ \ \beta_{\pi\pm} \simeq -3.4.$$

This value is still small in comparison with the existing data.

(2) The finite-mass correction is found to be surprisingly large for the charged-kaon electric polarizability: it takes $\alpha_{K\pm}$ from 0.8 (chiral limit) to 2.3. This is due to the strong mass dependence of the TBB (quark loop) contribution.

(3) We have found small and positive values for the electric polarizability of the neutral π and K. They appear to be about an order of magnitude smaller than their charged-meson counterparts, due to their vanishing nature in the chiral limit (with no meson loop). It is thus difficult for models to give a definite prediction of their signs although many models predict them to be negative (with or without the pion loop contribution). Experimentally, it is also difficult to determine the sign because the Thomson contribution to the Compton amplitude, which may be used as a reference for this purpose, is absent.

To conclude, we urge experimentalists to measure $\alpha_{\pi\pm}$ and $\alpha_{K\pm}$ with the best precision available to unravel the existing puzzle.

ACKNOWLEDGMENTS

One of us (T.M.) would like to thank A. Fonseca, G. C.-Branco, and members of CFNUL and GTAE at Lisbon, Portugal, for their warm hospitality. He is also grateful to J. Goity and G. Ecker for their instruction

in the rudiments of chiral perturbation theory, and to J. Villate and T. Girard for preparation and critical reading of the manuscript. The other (M.A.I.) would like to thank the Physics Department at VPI & SU, Theory Group at CEBAF, and CFNUL for their kind hospitality. Both of us acknowledge the partial support by the United States Department of Energy under Grant No. DE-FG-ER40413, Portuguese JNICT Grant No. PMCT/C/CEN/66/90, and CERN fund.

APPENDIX A: CALCULATIONAL TECHNIQUES

Let us consider the vector-vector quark loop (Fig. 1) to demonstrate certain calculational techniques of the diagrams in QCM. Here, we understand that the momenta are measured in units of Λ, and hence dimensionless. The integral corresponding to this diagram is

$$\Pi^{\mu\nu}_{VV}(p) = \int \frac{d^4k}{4\pi^2 i} \int d\sigma_v \, \mathrm{tr}[\gamma^\mu S_v(k)\gamma^\nu S_v(k+p)] = \int \frac{d^4k}{4\pi^2 i} \int d\sigma_v \, \mathrm{tr}\left(\gamma^\mu \frac{1}{v- \not{k}} \gamma_\nu \frac{1}{v- \not{k}- \not{p}}\right). \tag{A1}$$

By using the Feynman α parametrization, one obtains

$$\Pi^{\mu\nu}_{VV}(p) = \int \frac{d^4k}{\pi^2 i} \int d\sigma_v \int_0^1 \frac{2\alpha(1-\alpha)(g^{\mu\nu}p^2 - p^\mu p^\nu)}{[v^2 - k^2 - \alpha(1-\alpha)p^2]^2} = [g^{\mu\nu}p^2 - p^\mu p^\nu]\Pi_{VV}(p^2). \tag{A2}$$

We stress here that our confinement ansatz respects gauge invariance at each step of the calculation. The four-dimensional integral is evaluated by first going to the Euclidean region $k_0 \to ik_4$, $k^2 \to -k_E^2 \equiv -u$, then applying the prescription for the confinement ansatz [Eqs. (7)–(9)], in Sec. II. We thus find

$$\Pi_{VV}(p^2) = -2\int_0^1 d\alpha\,\alpha(1-\alpha)\int_0^\infty u\,du \;\frac{d}{du}\int d\sigma_v \frac{1}{v^2+u-\alpha(1-\alpha)p^2} = 2\int_0^1 d\alpha\,\alpha(1-\alpha)\int_0^\infty du\, b[u-\alpha(1-\alpha)p^2] = \frac{1}{3}R_V(p^2), \tag{A3}$$

where

$$R_V(x) \equiv \int_0^\infty du\, b(u) + \frac{x}{4}\int_0^1 du\, b\left(-u\frac{x}{4}\right)\sqrt{1-u}\left(1+\frac{u}{2}\right) = B_0 + \frac{x}{4}\int_0^1 du\, b\left(-u\frac{x}{4}\right)\sqrt{1-u}\left(1+\frac{u}{2}\right). \tag{A4}$$

APPENDIX B: QUARK-MESON COUPLING CONSTANTS

In this appendix the effective coupling constants $h_H = 3g_H^2/4\pi^2$ for various mesons appearing in Sec. II are given. They are obtained from the compositeness condition [Eq. (2)], together with the derivative of mass operators obtained in a way similar to the example given in the preceding appendix. Here again, $\mu_P \equiv m_P/\Lambda$.

(1) Pseudoscalar mesons $J^{PC} = 0^{-+}$, $P = (\pi, K, \eta, \eta')$:

$$h_P^{-1} = \frac{1}{2}R_{PP}(\mu_P^2), \tag{B1}$$

where

$$R_{PP}(x) = B_0 + \frac{x}{4}\int_0^1 du\, b\left(-\frac{ux}{4}\right)\frac{1-u/2}{\sqrt{1-u}}. \tag{B2}$$

(2) Scalar mesons $J^{PC} = 0^{++}$, $S = (a_0, K_0, f_0, \varepsilon)$:

$$h_S^{-1} = \frac{1}{2}[R^{(0)}_{SS}(\mu_S^2) + 4H R^{(1)}_{SS}(\mu_S^2) - 4H^2 R^{(2)}_{SS}(\mu_S^2)], \tag{B3}$$

where

$$R^{(0)}_{SS}(x) = B_0 + \frac{x}{4}\int_0^1 du\, b\left(-\frac{ux}{4}\right)(1+u/2)\sqrt{1-u}, \tag{B4}$$

$$R^{(1)}_{SS}(x) = A_0 + \frac{x}{4}\int_0^1 du\, a\left(-\frac{ux}{4}\right)(1+u/2)\sqrt{1-u}), \tag{B5}$$

and

$$R^{(2)}_{SS}(x) = B_1 - \frac{x^2}{16}\int_0^1 u\,du\, b\left(-\frac{ux}{4}\right)(1+u/2)\sqrt{1-u}. \tag{B6}$$

(3) Vector mesons $J^{PC} = 1^{--}$, $V = (\rho, K^*, \omega, \phi)$:

$$h_V^{-1} = \frac{1}{3}R_{VV}(\mu_V^2), \tag{B7}$$

with

$$R_{VV}(x) = B_0 + \frac{x}{4}\int_0^1 du\, b\left(-\frac{ux}{4}\right)\frac{(1-u/2+u^2/4)}{\sqrt{1-u}}. \tag{B8}$$

(4) Axial-vector mesons $J^{PC} = 1^{++}$, $A = (a_1, K_1, f_1)$:

$$h_A^{-1} = \frac{1}{3}R_{AA}(\mu_A^2), \tag{B9}$$

where

$$R_{AA}(x) = B_0 + \frac{x}{4}\int_0^1 du\, b\left(-\frac{ux}{4}\right)(1+u/2)\sqrt{1-u}. \tag{B10}$$

APPENDIX C: QCM CALCULATION OF THE INVARIANT COMPTON AMPLITUDE

We give below some details of the calculation of the invariant Compton amplitudes, the result of which is presented in Sec. III. The amplitude is defined by diagrams in Figs. 5–7.

1. TBB diagrams

The most cumbersome calculations are required for box diagrams. Here again, we assume for simplicity that all the momenta are given in units of Λ. The structure integral corresponding to the diagram Fig. 5(a) is written in the form

$$\begin{aligned}
I^{\mu\nu}_{\Box a} &= \int \frac{d^4k}{4\pi^2 i}\int d\sigma_v\ \mathrm{tr}[\gamma^\mu S_v(k)\gamma^\nu S_v(k+q_2)\gamma^5 S_v(k+q_1+p_1)\gamma^5 S_v(k+q_1)] + \text{cross terms} \\
&= g^{\mu\nu}R_{PP}(\mu_P^2) + \int_0^1 \frac{dv}{\sqrt{1-v}} b\left(-v\frac{\mu_P^2}{4}\right)\left(-\frac{v}{4}K^{\mu\nu} - \frac{v}{8}\tilde{T}_2^{\mu\nu}\right) \\
&\quad - \int_0^1 \frac{dv}{\sqrt{1-v}} b'\left(-v\frac{\mu_P^2}{4}\right)\left[\frac{1}{12}L^{\mu\nu} - \frac{v^2}{16}\left(q_1\cdot q_2 + \frac{\mu_P^2}{2}\right)(q_2^\mu p_2^\nu + p_1^\mu q_1^\nu - 2p_1^\mu p_2^\nu)\right. \\
&\qquad \left. + \frac{v^2}{64}\mu_P^2\tilde{T}_2^{\mu\nu} + \frac{v^2}{16}\left(p_1\cdot q_1(p_1\cdot q_1 - q_1\cdot q_2) + (q_1\cdot q_2)^2 + \frac{\mu_P^2}{2}q_1\cdot q_2\right)g^{\mu\nu}\right] \\
&\quad + \mu_P^2\int_0^1 \frac{dv}{\sqrt{1-v}} b''\left(-v\frac{\mu_P^2}{4}\right)\left[\left(\frac{v^3}{384} - \frac{v^2}{64} + \frac{v}{48}\right)L^{\mu\nu} - \frac{v^2(1-v)}{192}\mu_P^2\tilde{T}_2^{\mu\nu} - \frac{v^3}{192}N^{\mu\nu}\right],
\end{aligned} \tag{C1}$$

where $\tilde{T}_2^{\mu\nu}$ is one of the two gauge-invariant Lorentz tensors found in the defining equation of the Compton amplitude in Sec. III [Eqs. (22) and (23)], whereas

$$K^{\mu\nu} \equiv q_2^\mu p_2^\nu + p_1^\mu q_1^\nu - 2p_1^\mu p_2^\nu - g^{\mu\nu}q_1 q_2, \tag{C2}$$

$$L^{\mu\nu} \equiv q_2^\mu p_2^\nu p_1\cdot q_1 + p_1^\mu q_1^\nu p_1\cdot q_1 - p_1^\mu p_2^\nu q_1\cdot q_2 - g^{\mu\nu}(p_1\cdot q_1)^2 = \tilde{T}_1^{\mu\nu}m_P^2, \tag{C3}$$

and

$$N^{\mu\nu} \equiv q_1\cdot q_2(q_2^\mu p_2^\nu + p_1^\mu q_1^\nu - 2p_1^\mu p_2^\nu) - g^{\mu\nu}[p_1\cdot q_1(p_1\cdot q_1 - q_1\cdot q_2) + (q_1\cdot q_2)^2]. \tag{C4}$$

The function $R_{PP}(x)$ is found in Appendix B.

The structure integral corresponding to diagram Fig. 5(b) is written as

$$\begin{aligned}
I^{\mu\nu}_{\Box b} &= \int \frac{d^4k}{4\pi^2 i}\int d\sigma_v\ \mathrm{tr}[\gamma^\mu S_v(k+p_1)\gamma^5 S_v(k)\gamma^\nu S_v(k+q_2)\gamma^5 S_v(k+p_1+q_1)] + \text{cross terms} \\
&= -2g^{\mu\nu}R_{PP}(\mu_P^2) + \int_0^1 \frac{dv}{\sqrt{1-v}} b\left(-v\frac{\mu_P^2}{4}\right)\left(\frac{v}{2}K^{\mu\nu} + \frac{3v}{4}\tilde{T}_2^{\mu\nu}\right) \\
&\quad - \int_0^1 \frac{dv}{\sqrt{1-v}} b'\left(-v\frac{\mu_P^2}{4}\right)\left[\frac{v^2}{8}\left(q_1\cdot q_2 + \frac{\mu_P^2}{2}\right)(q_2^\mu p_2^\nu + p_1^\mu q_1^\nu - 2p_1^\mu p_2^\nu)\right. \\
&\qquad \left. - \frac{v^2}{8}\left(p_1\cdot q_1(p_1\cdot q_1 - q_1\cdot q_2) + (q_1\cdot q_2)^2 + \frac{\mu_P^2}{2}q_1\cdot q_2\right)g^{\mu\nu} + \frac{5v^2}{32}\mu_P^2\tilde{T}_2^{\mu\nu}\right] \\
&\quad + \mu_P^2\int_0^1 \frac{dv}{\sqrt{1-v}} b''\left(-v\frac{\mu_P^2}{4}\right)\left(-\frac{v^3}{192}L^{\mu\nu} + \frac{v^3}{96}N^{\mu\nu}\right),
\end{aligned} \tag{C5}$$

where $K^{\mu\nu}$, $L^{\mu\nu}$, $N^{\mu\nu}$ have already been defined above.

For neutral mesons the invariant Compton amplitude receives contributions only from these two box diagrams. The resulting amplitude is

$$M^{\mu\nu}_{\mathrm{TBB}\ P^0} = e^2 h_P C_P (2 I^{\mu\nu}_{\Box a} + I^{\mu\nu}_{\Box b}), \tag{C6}$$

where C_P is 5/18 for π^0, and 1/9 for K_0, respectively.

For charged mesons the Compton scattering is represented by diagrams in Fig. 5(d). Here the first three triangle + bubble (TB) diagrams give the contribution,

$$M^{\mu\nu}_{\mathrm{TB}} = M^{\mu\nu}_{\mathrm{point}} - 2e^2 g^{\mu\nu} + \tilde{M}^{\mu\nu}_{\mathrm{TB\text{-}SD}}, \tag{C7}$$

where the first term is for the scattering by a point charge [identical to the expression in Eq. (20)], whereas the third term, which is structure dependent, we write as

$$\tilde{M}^{\mu\nu}_{\mathrm{TB\text{-}SD}} = e^2 h_P I^{\mu\nu}_{\mathrm{TB}}. \tag{C8}$$

In the above expression

$$\begin{aligned} I^{\mu\nu}_{TB} = & \int_0^1 \frac{dv}{\sqrt{1-v}} b\left(-v\frac{\mu_P^2}{4}\right)\left(\frac{v}{4}K^{\mu\nu} + \frac{v}{4}\tilde{T}_2^{\mu\nu}\right) \\ & - \int_0^1 \frac{dv}{\sqrt{1-v}} b'\left(-v\frac{\mu_P^2}{4}\right)\left[-\frac{v^2}{16}L^{\mu\nu} + \frac{v^2}{16}\left(q_1q_2 + \frac{\mu_P^2}{2}\right)(q_2^\mu p_2^\nu + p_1^\mu q_1^\nu - 2p_1^\mu p_2^\nu)\right. \\ & \left. - \frac{v^2}{16}\left(p_1q_1(p_1q_1 - q_1q_2) + (q_1q_2)^2 + \frac{\mu_P^2}{2}q_1q_2\right)g^{\mu\nu} + \frac{v^2}{32}\mu_P^2\tilde{T}_2^{\mu\nu}\right] \\ & + \mu_P^2 \int_0^1 \frac{dv}{\sqrt{1-v}} b''\left(-v\frac{\mu^2}{4}\right)\left(-\frac{v^3}{192}L^{\mu\nu} + \frac{v^3}{192}N^{\mu\nu}\right). \end{aligned} \tag{C9}$$

The total TBB contribution to the charged-particle Compton amplitude is then written as

$$M^{\mu\nu}_{\mathrm{TBB}+} = M^{\mu\nu}_{\mathrm{point}} - 2e^2 g^{\mu\nu} + e^2 h_P (I^{\mu\nu}_{\mathrm{TB}} + 5/9 I^{\mu\nu}_{\Box a} - 2/9 I^{\mu\nu}_{\Box b}). \tag{C10}$$

With a little algebra and by recovering the correct dimension, we obtain the invariant Compton amplitude at threshold from TBB.

(i) Neutral mesons

$$M^{\mu\nu}_{\mathrm{TBB}\pi^0} = \frac{e^2 h_\pi}{\Lambda^2}[\mu_\pi^2 \tilde{T}_1^{\mu\nu} W_1^{(0)}(\mu_\pi^2) + \tilde{T}_2^{\mu\nu} W_2^{(0)}(\mu_\pi^2)], \tag{C11}$$

and

$$M^{\mu\nu}_{\mathrm{TBB}K^0} = \frac{2e^2 h_K}{5\Lambda^2}[\mu_K^2 \tilde{T}_1^{\mu\nu} W_1^{(0)}(\mu_K^2) + \tilde{T}_2^{\mu\nu} W_2^{(0)}(\mu_K^2)]. \tag{C12}$$

(ii) Charged mesons

$$M^{\mu\nu}_{\mathrm{TBB}+} = M^{\mu\nu}_{\mathrm{point}} + M^{\mu\nu}_{+\mathrm{SD}}. \tag{C13}$$

Here, as before, the first term is the point charge contribution while the second is structure dependent and may be written as

$$M^{\mu\nu}_{+SD} = \frac{e^2 h_P}{\Lambda^2}[\mu_P^2 \tilde{T}_1^{\mu\nu} W_1^{(+)}(\mu_P^2) + \tilde{T}_2^{\mu\nu} W_2^{(+)}(\mu_P^2)]. \tag{C14}$$

The $W(x)$'s are

$$W_1^0(x) = \frac{5}{108}\left[B - \int_0^1 \frac{du}{\sqrt{1-u}} b'\left(-\frac{ux}{4}\right) + \frac{x}{4}\int_0^1 \frac{du}{\sqrt{1-u}} b''\left(-\frac{ux}{4}\right)\left(u - \frac{3}{4}u^2\right)\right], \tag{C15}$$

with

$$W_1^0(0) = -\frac{5}{54}b'(0),$$

$$W_2^0(x) = \frac{5}{36}\left[\int_0^1 \frac{du}{\sqrt{1-u}} b\left(-\frac{ux}{4}\right)u - \frac{x}{4}\int_0^1 \frac{du}{\sqrt{1-u}} b'\left(-\frac{ux}{4}\right)\frac{3}{2}u^2 - \frac{x^2}{16}\int_0^1 \frac{du}{\sqrt{1-u}} b''\left(-\frac{ux}{4}\right)\frac{u^2(1-u)}{3}\right], \tag{C16}$$

with

$$W_2^0(0)=\frac{5}{27}b(0),$$

$$W_1^+(x)=\frac{5}{108}\left[-\int_0^1\frac{du}{\sqrt{1-u}}b'\left(-\frac{ux}{4}\right)\left(1-\frac{27}{4}u^2\right)+\frac{x}{4}\int_0^1\frac{du}{\sqrt{1-u}}b''\left(-\frac{ux}{4}\right)u\left(1-\frac{u}{4}\right)\right], \tag{C17}$$

with

$$W_1^+(0)=\frac{7}{270}b'(0),$$

and

$$W_2^+(x)=\frac{1}{72}\left[\int_0^1\frac{du}{\sqrt{1-u}}b\left(-\frac{ux}{4}\right)u-\frac{x}{4}\int_0^1\frac{du}{\sqrt{1-u}}b'\left(-\frac{ux}{4}\right)\frac{3}{2}u^2-\frac{x^2}{16}\int_0^1\frac{du}{\sqrt{1-u}}b''\left(-\frac{ux}{4}\right)6u^2(1-u)\right], \tag{C18}$$

with

$$W_2^+(0)=\frac{1}{54}b(0).$$

2. The scalar mesons

The contribution of t-channel scalar-meson exchanges to the Compton amplitude is defined by the diagram in Fig. 6(a). The invariant matrix element is written in the form

$$M_S^{\mu\nu}=-e^2h_Ph_S\frac{1}{4}C_{SPP}C_{S\gamma\gamma}\tilde{F}_{SPP}[(p_1-p_2)^2;p_1^2;p_2^2]D_S[(p_1-p_1)^2]F_{S\gamma\gamma}^{\mu\nu}(-q_1;q_2)+\text{cross terms}. \tag{C19}$$

Here the function F_{SPP} corresponding to the decay $S\to PP$ is written as

$$\tilde{F}_{SPP}(p^2;p_1^2;p_2^2)=\int\frac{d^4k}{4\pi^2i}\int d\sigma_v\,\mathrm{tr}\left[\left(1+\frac{H}{\Lambda}(2\not{k}+\not{p}_2-\not{p}_1)\right)S_v(k-p_1)\gamma^5S_v(k)\gamma^5S_v(k+p_2)\right]$$
$$=\Lambda F_{SPP}\left(\frac{p^2}{\Lambda^2},\frac{p_1^2}{\Lambda^2},\frac{p_2^2}{\Lambda^2}\right), \tag{C20}$$

where

$$F_{SPP}(x,y,z)\equiv F_{SPP}^{(1)}(x,y,z)-4HF_{SPP}^{(2)}(x,y,z). \tag{C21}$$

The expression for this function is rather lengthy, but for our present purpose the following particular cases are sufficient:

$F_{SPP}^{(1)}(x,0,0)$

$$=A_0-\frac{x}{4}\int_0^1du\,a\left(-\frac{ux}{4}\right)\times\left(\frac{1}{2}\ln\frac{1+\sqrt{1-u}}{1-\sqrt{1-u}}-\sqrt{1-u}\right), \tag{C22}$$

$F_{SPP}^{(2)}(x,0,0)$

$$=B_1+\frac{x^2}{32}\int_0^1du\,ub\left(-\frac{ux}{4}\right)\times\left(\frac{1}{2}\ln\frac{1+\sqrt{1-u}}{1-\sqrt{1-u}}-\sqrt{1-u}\right), \tag{C23}$$

$$F_{SPP}^{(1)}(0,x,x)=A_0+\frac{x}{4}\int_0^1\frac{du}{\sqrt{1-u}}a\left(-\frac{ux}{4}\right), \tag{C24}$$

and

$$F_{SPP}^{(2)}(0,x,x)=B_1+\frac{x}{4}\left[B_0+\frac{x}{4}\int_0^1du\,b\left(-\frac{ux}{4}\right)\frac{1-3u/2}{\sqrt{1-u}}\right]. \tag{C25}$$

Here we adopt the free propagator for the scalar field:

$$D_S(p^2)=\frac{1}{m_S^2-p^2}.$$

The function $F_{S\gamma\gamma}$ defining the decay $S\to\gamma\gamma$ is written as

$$F^{\mu\nu}_{S\gamma\gamma}(q_1;q_2)=\int\frac{d^4k}{4\pi^2 i}\int d\sigma_v\,\mathrm{tr}\left[\left(1+\frac{H}{\Lambda}(2\not{k}+\not{q}_2-\not{q}_1)\right)S_v(k-q_1)\gamma^\mu S_v(k)\gamma^\nu S_v(k+q_2)\right]$$

$$=\frac{1}{\Lambda}(g^{\mu\nu}q_1\cdot q_2-q_1^\nu q_2^\mu)F_{S\gamma\gamma}\left(\frac{p^2}{\Lambda^2}\right), \tag{C26}$$

where

$$F_{S\gamma\gamma}(x)\equiv F^{(1)}_{S\gamma\gamma}(x)+HF^{(2)}_{S\gamma\gamma}(x), \tag{C27}$$

$$F^{(1)}_{S\gamma\gamma}(x)=\frac{1}{4}\int_0^1 du\,a\left(-\frac{ux}{4}\right)(1-u)\ln\frac{1+\sqrt{1-u}}{1-\sqrt{1-u}}, \tag{C28}$$

$$F^{(2)}_{S\gamma\gamma}(x)=\frac{x}{8}\int_0^1 du\,b\left(-\frac{ux}{4}\right)u(1-u)\ln\frac{1+\sqrt{1-u}}{1-\sqrt{1-u}}, \tag{C29}$$

and

$$F_{S\gamma\gamma}(0)=\frac{a(0)}{3}. \tag{C30}$$

Next we collect the SU(3) factors $C_{SPP'}$ and $C_{S\gamma\gamma}$,

$$C_{SPP'}=\mathrm{tr}[\lambda^S\{\lambda^P,(\lambda^{P'})^\dagger\}],$$

and, more concretely,

$$C_{S\pi\pi}=\begin{cases}4\cos\delta_S & (\varepsilon),\\ -4\sin\delta_S & (f_0),\end{cases}$$

$$C_{SKK}=\begin{cases}2(\cos\delta_S-\sqrt{2}\sin\delta_S) & (\varepsilon),\\ -2(\sin\delta_S+\sqrt{2}\cos\delta_S) & (f_0),\end{cases}$$

$$C_{a_0K^+K^-}=2,\quad C_{a_0K^0\bar{K}^0}=-2.$$

The factor $C_{S\gamma\gamma}$ is equal to

$$C_{S\gamma\gamma}=\mathrm{tr}[\lambda^S(\lambda^Q)^2]=\begin{cases}\frac{1}{9}(5\cos\delta_S-\sqrt{2}\sin\delta_S) & (\varepsilon),\\ -\frac{1}{9}(5\sin\delta_S+\sqrt{2}\cos\delta_S) & (f_0),\\ \frac{1}{3} & (a_0),\end{cases}$$

where λ^Q is the diagonal quark charge matrix. Finally, we obtain the contribution at threshold:

$$M^{\mu\nu}_S=\tilde{T}^{\mu\nu}_2\frac{-e^2h_P}{2\Lambda^2}\times C_{SPP}F_{SPP}(0,\mu_P^2,\mu_P^2)C_{S\gamma\gamma}F_{S\gamma\gamma}(0)h_S/\mu_S^2. \tag{C31}$$

3. Axial mesons

First of all, let us consider the decay $A\to P\gamma$. This is defined by diagrams Figs. 10(a)–10(c). The contribution of the triangle diagram [Fig. 10(a)] may be written as

$$M^{(a)}(A\to P\gamma)=-ie\sqrt{h_Ah_P}(\tfrac{1}{2}C_{AP\gamma})\Lambda\epsilon_A^\alpha\epsilon_\gamma^\mu F^{\alpha\mu}_{APV}(p,q), \tag{C32}$$

where ϵ_A and ϵ_γ are the polarizations vectors of the axial-vector mesons and photon, respectively. For the axial-vector meson on the mass shell we have

$$p_A^2=(p+q)^2=m_A^2,\quad p^2=m_P^2,$$
$$q^2=0,\quad(\epsilon_A\cdot p_A)=(\epsilon_\gamma\cdot q)=0. \tag{C33}$$

The SU(3) factors are

$$C_{AP\gamma}=\mathrm{tr}\{\lambda^A[(\lambda^P)^\dagger,\lambda^Q]\}=\mathrm{tr}\{\lambda^Q[\lambda^A,(\lambda^P)^\dagger]\}=\begin{cases}2 & (\text{charged}),\\ 0 & (\text{neutral}).\end{cases}$$

The structure function $F^{\alpha\mu}_{APV}(p,q)$ is equal to

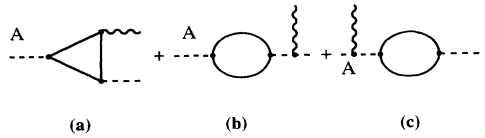

FIG. 10. Diagrams describing axial-meson decay $A\to P\gamma$.

$$F^{\alpha\mu}_{APV}(p,q)=\frac{1}{\Lambda}\int\frac{d^4k}{4\pi^2 i}\int d\sigma_v\,\mathrm{tr}[\gamma^\alpha\gamma^5 S_v(k-p)\gamma^5 S_v(k)\gamma^\mu S_v(k+q)]$$
$$=g^{\alpha\mu}F_{AP}(\mu_A^2)-2p^\mu q^\alpha\frac{F_{AP}(\mu_A^2)-F_{AP}(\mu_P^2)}{m_A^2-m_P^2}+(q^\alpha p^\mu-g^{\alpha\mu}p\cdot q)\frac{\mu_A^2R_{PVV}(\mu_A^2)-\mu_P^2R_{PVV}(\mu_P^2)}{m_A^2-m_P^2}, \tag{C34}$$

where

$$F_{AP}(x)=A_0+\frac{x}{4}\int_0^1 du\,a\left(-u\frac{x}{4}\right)\sqrt{1-u} \tag{C35}$$

and

$$R_{PVV}(x)=\frac{1}{4}\int_0^1 du\,a\left(-u\frac{x}{4}\right)\ln\left(\frac{1+\sqrt{1-u}}{1-\sqrt{1-u}}\right). \tag{C36}$$

The contribution of the diagram in Fig.10(b) is

$$M^{(b)}(A\to P\gamma)=-ie\sqrt{h_Ah_P}\Lambda\epsilon_A^\alpha\epsilon_\gamma^\mu[-(p+q)^\mu D_A^{\alpha\beta}(p)-p^\mu D_A^\alpha(p)+g^{\mu\alpha}(p+q)^\nu D_A^{\nu\beta}(p)+p^\alpha D_A^{\mu\beta}(p)]F_{AP}^\beta(p), \tag{C37}$$

where the structure integral $F_{AP}^\beta(p)$ is equal to

$$F_{AP}^\beta(p)=\frac{1}{\Lambda}\int\frac{d^4k}{4\pi^2 i}\int d\sigma_v\,\mathrm{tr}[\gamma^\beta\gamma^5 S_v(k)\gamma^5 S_v(k+p)]=p^\beta F_{AP}\left(\frac{p^2}{\Lambda^2}\right), \tag{C38}$$

and the free axial propagator is

$$D_A^{\alpha\beta}(p)=\frac{-g^{\alpha\beta}+p^\alpha p^\beta/m_A^2}{m_A^2-p^2}. \tag{C39}$$

The contribution of the diagram in Fig. 10(c) is written as

$$M^{(c)}(A\to P\gamma)=-2ie\sqrt{h_Ah_P}\Lambda\epsilon_A^\alpha\epsilon_\gamma^\mu[(p+q)^\alpha p^\mu]\frac{F_{AP}(\mu_A^2)}{\mu_P^2-\mu_A^2}, \tag{C40}$$

which vanishes when the axial-vector meson is on its mass shell.

Finally, we get the gauge-invariant form for the invariant matrix element

$$M(A\to P\gamma)=-ie\frac{G_{AP\gamma}}{m_A^2}\epsilon_A^\alpha\epsilon_\gamma^\mu(g^{\alpha\mu}pq-q^\alpha p^\mu), \tag{C41}$$

where

$$G_{AP\gamma}=\sqrt{h_Ah_P}\Lambda\mu_A^2\left(\frac{1}{\mu_A^2}F_{AP}(\mu_P^2)+\frac{2[F_{AP}(\mu_A^2)-F_{AP}(\mu_P^2)]-[\mu_A^2R_{PVV}(\mu_A^2)-\mu_P^2R_{PVV}(\mu_P^2)]}{\mu_A^2-\mu_P^2}\right)$$
$$=\sqrt{h_Ah_P}\Lambda\mu_A^2\left(\frac{1}{\mu_A^2}F_{AP}(\mu_P^2)+F_{AP\gamma}(\mu_A^2,\mu_P^2)\right). \tag{C42}$$

Here function $F_{AP\gamma}(x,y)$ is defined as

$$F_{AP\gamma}(x,y)=\frac{xR_{AP\gamma}(x)-yR_{AP\gamma}(y)}{x-y}, \tag{C43}$$

where

$$R_{AP\gamma}(x)=\frac{1}{4}\int_0^1 du\,a\left(-u\frac{x}{4}\right)\times\left[2\sqrt{1-u}-\ln\left(\frac{1+\sqrt{1-u}}{1-\sqrt{1-u}}\right)\right]. \tag{C44}$$

The first term in the expression for $G_{AP\gamma}$ can be neglected because $1/\mu_A^2\sim 0.1$. In this approximation we have

$$G_{AP\gamma}=\sqrt{h_Ah_P}\Lambda\mu_A^2F_{AP\gamma}(\mu_A^2,\mu_P^2)$$
$$\simeq\sqrt{h_Ah_P}\Lambda\mu_A^2R_{AP\gamma}(\mu_A^2). \tag{C45}$$

In the above expression, we have neglected the pseudoscalar-meson mass relative to that for the axial-vector meson.

We next calculate the radiative decay width for $a_1\to\pi\gamma$. This is equal to

$$\Gamma(a_1\to\pi\gamma)=\frac{\alpha}{24}\frac{G_{a_1\pi\gamma}^2}{m_{a_1}}. \tag{C46}$$

The numerical result is shown in Table. III.

Now, let us consider the contribution of intermediate axial vector mesons to the polarizabilities of pseudoscalar mesons. As mentioned above, we will neglect the terms proportional to $1/\mu_A^2$ which come mainly from the diagrams containing two or more axial vector meson propagators. In this approximation only the diagrams of Figs. 7(a)–7(d) are important.

The invariant matrix element corresponding to these diagrams is written in the form

$$\begin{aligned} M_A^{\mu\nu} = & - e^2 h_P h_A [F_{APV}^{\alpha\mu}(-p_1,-q_1) - g^{\alpha\mu} F_{AP}(p_1^2)] \\ & \times D^{\alpha\beta}(p_1+q_1) \\ & \times [F_{APV}^{\beta\nu}(p_2,q_2) - g^{\beta\nu} F_{AP}(p_2^2)] + \text{cross terms}. \end{aligned} \tag{C47}$$

This can be calculated from what we have obtained above. The final result for the axial vector meson contribution to the threshold Compton amplitude is

$$M_A^{\mu\nu} = \tilde{T}_1^{\mu\nu} \frac{e^2 h_P}{\Lambda^2} \mu_P^2 F_{AP\gamma}^2(\mu_P^2,\mu_P^2) \left(\frac{h_A}{\mu_A^2 - \mu_P^2} + \frac{h_A}{\mu_A^2} \right). \tag{C48}$$

4. Vector mesons

The contribution of vector mesons to the Compton amplitude is shown in Fig. 6(b). The invariant matrix element for the s-channel exchange is written in the form

$$\begin{aligned} M_V^{\mu\nu} = & - e^2 h_P h_V (\tfrac{1}{4} C_{VP\gamma}^2) F_{PVV}^{\mu\alpha} \\ & \times (-q_1; p_1+q_1) D_V^{\alpha\beta}(p_1+q_1) \\ & \times F_{PVV}^{\beta\nu}(-(p_2+q_2); q_2) + \text{cross terms}. \end{aligned} \tag{C49}$$

Here, the function $F^{\mu\nu}(q_1;q_2)$ corresponding to the decay $P \to VV$ is

$$\begin{aligned} F_{PVV}^{\mu\nu}(q_1;q_2) = & \int \frac{d^4k}{4\pi^2 i} \int d\sigma_v \mathrm{tr}\, [\gamma^5 S_v(k-q_1) \\ & \times \gamma^\mu S_v(k) \gamma^\nu S_v(k+q_2)]. \end{aligned} \tag{C50}$$

With the symmetry property of this function,

$$F_{PVV}^{\mu\nu}(q_1,q_2) = F_{PVV}^{\nu\mu}(q_2,q_1), \tag{C51}$$

it may then be written as

$$F_{PVV}^{\mu\nu} = (i/\Lambda) \epsilon^{\mu\nu\alpha\beta} q_1^\alpha q_2^\beta F_{PVV} \left(\frac{(q_1+q_2)^2}{\Lambda^2}, \frac{q_1^2}{\Lambda^2}, \frac{q_2^2}{\Lambda^2} \right). \tag{C52}$$

The function F_{PVV} for general arguments takes a rather complicated form, but for our purpose the following particular cases are sufficient:

$$\begin{aligned} F_{PVV}(x,0,0) \equiv & R_{PVV}(x) \\ = & \frac{1}{4} \int_0^1 a\left(-v\frac{x}{4}\right) \ln \frac{1+\sqrt{1-v}}{1-\sqrt{1-v}}, \end{aligned} \tag{C53}$$

$$F_{PVV}(x,y,0) = \frac{x R_{PVV}(x) - y R_{PVV}(y)}{x-y}, \tag{C54}$$

$$F_{PVV}(x,x,0) = \frac{1}{4} \int_0^1 \frac{dv}{\sqrt{1-v}} a\left(-v\frac{x}{4}\right). \tag{C55}$$

The free propagator of vector field is

$$D_V^{\alpha\beta}(p) = \frac{-g^{\alpha\beta} + p^\alpha p^\beta / m_V^2}{m_V^2 - p^2}. \tag{C56}$$

The SU(3) factor $C_{VP\gamma}$ is equal to

$$C_{VP\gamma} = \mathrm{tr}[\lambda^Q \{\lambda^P, (\lambda^V)^\dagger\}].$$

In particular, we obtain

$$C_{\rho\pi\gamma} = \tfrac{1}{9}, \quad C_{\omega\pi\gamma} = 1, \quad C_{K^{*+}K^+\gamma} = \tfrac{1}{9}, \quad C_{K^{*0}K^0\gamma} = \tfrac{4}{9}.$$

Performing the convolution of antisymmetric tensors and taking into account the cross diagram, we obtain the final result

$$\begin{aligned} M_V^{\mu\nu} = & (\tilde{T}_1^{\mu\nu} + \tilde{T}_2^{\mu\nu}) \frac{e^2 h_P}{4\Lambda^2} \mu_P^2 C_{VP\gamma}^2 F_{PVV}(\mu_P^2,\mu_P^2,0) \\ & \times \left(\frac{h_V}{\mu_V^2 - \mu_P^2} + \frac{h_V}{\mu_V^2} \right). \end{aligned} \tag{C57}$$

[1] V. A. Petrunkin, Fiz. Elem. Chastits At. Yadra **12**, 692 (1981) [Sov. J. Part. Nucl. **12**, 278 (1981)].

[2] J. L. Friar, in *Electron-Nucleus Scattering*, Proceedings of the Workshop, Marciana Marina, Italy, 1988, edited by A. Fabrocini *et al.* (World Scientific, Singapore, 1989), p. 3.

[3] B. R. Holstein, Commun. Nucl. Part. Phys. **19**, 221 (1990).

[4] M. A. Moinester and M. Blecher, in Proceedings of the Workshop on Science at the KAON Factory, Vancouver, Canada, 1990, edited by D. Gill (unpublished), Vol. 2.

[5] M. V. Terent'ev, Yad. Fiz. **16**, 167 (1973) [Sov. J. Nucl. Phys. **16**, 87 (1973)]; **19**, 1298 (1974) [**19**, 664 (1974)].

[6] E. Llanta and R. Tarrach, Phys. Lett. **91B**, 132 (1980).

[7] D. Ebert and M. K. Volkov, Phys. Lett. **101B**, 252 (1981).

[8] A. I. L'vov, Yad. Fiz. **36**, 494 (1982) [Sov. J. Nucl. Phys. **36**, 289 (1982)].

[9] M. K. Volkov and A. A. Osipov, Yad. Fiz. **41**, 1027 (1985) [Sov. J. Nucl. Phys. **41**, 659 (1985)].

[10] M. K. Volkov and V. N. Pervushin, Yad. Fiz. **22**, 346 (1975) [Sov. J. Nucl. Phys. **22**, 179 (1976)].

[11] V. Bernard, B. Hiller, and W. Weise, Phys. Lett. B **205**, 16 (1988).

[12] A. I. L'vov and V. A. Petrunkin, Kratk. Soobschch. Fiz. **12**, 39 (1985).

[13] L. V. Fil'kov, I. Guiasu, and E. E. Radescu, Phys. Rev. D **26**, 3146 (1982).
[14] Particle Data Group, J. J. Hernández *et al.*, Phys. Lett. B **239**, 1 (1990).
[15] Yu. M. Antipov *et al.*, Phys. Lett. **121B**, 445 (1983); Z. Phys. C **26**, 495 (1985).
[16] J. Gasser and H. Leutwyler, Ann. Phys. (N.Y.) **158**, 142 (1984); Nucl. Phys. **B250**, 465 (1985).
[17] J. Balog, Phys. Lett. **149B**, 197 (1984); D. Ebert and H. Reinhardt, Nucl. Phys. **B271**, 188 (1986).
[18] J. F. Donoghue and B. R. Holstein, Phys. Rev. D **40**, 2378 (1989).
[19] G. V. Efimov and M. A. Ivanov, Int. J. Mod. Phys. A **4**, 2031 (1989); Fiz. Elem. Chastits At. Yadra **20**, 1129 (1989) [Sov. J. Part. Nucl. **20**, 479 (1989)]; G. V. Efimov, M. A. Ivanov, and V. E. Lyubovitskii, Z. Phys. C **47**, 583 (1990).
[20] E. Z. Avakian, S. L. Avakyan, G. V. Efimov, and M. A. Ivanov, Yad. Fiz. **49**, 1398 (1989) [Sov. J. Nucl. Phys. **49**, 867 (1989)].
[21] M. K. Volkov and D. Ebert, Yad. Fiz. **36**, 1265 (1982) [Sov. J. Nucl. Phys. **36**, 736 (1982)]; M. K. Volkov and D. V. Kreopalov, *ibid.* **39**, 924 (1984) [**39**, 585 (1984)].
[22] E. B. Dally *et al.*, Phys. Rev. Lett. **48**, 375 (1982).
[23] V. De Alfaro *et al.*, *Currents in Hadron Physics* (North-Holland, Amsterdam, 1976).
[24] R. Machleidt, K. Holinde, and Ch. Elster, Phys. Rep. **149**, 1 (1987).
[25] J. Weinstein and N. Isgur, Phys. Rev D **27**, 588 (1983).
[26] R. L. Jaffe, Phys. Rev. D **17**, 1444 (1978); N. N. Achasov, S. A. Devyanin, G. N. Shestakov, Usp. Fiz. Nauk **142**, 361 (1984) [Sov. Phys. Usp. **27**, 161 (1984)].
[27] J. Ellis and J. Lanik, Phys. Lett. B **175**, 83 (1983).
[28] A. A. Bel'kov *et al.*, *Pion-Pion Interaction* (Energoatomizdat, Moscow, 1985).
[29] G. V. Efimov, M. A. Ivanov, and S. G. Mashnik, Report No. JINR E2-89-780, Dubna, 1989 (unpublished).
[30] G. Feinberg and J. Sucher, Phys. Rev. A **2**, 2395 (1970).
[31] V. A. Petrunkin, Nucl. Phys. **55**, 197 (1964).
[32] J. L. Friar, Ann. Phys. (N.Y.) **95**, 170 (1975).
[33] T. E. O. Ericson and J. Hüfner, Nucl. Phys. **B47**, 205 (1972).
[34] C. Itzykson and J.-B. Zuber, *Quantum Field Theory* (McGraw-Hill, New York, 1980).
[35] A. I. L'vov and V. A. Petrunkin, Report No. 170, Lebedev Physics Institute, 1977 (unpublished).
[36] J. F. Donoghue, B. R. Holstein, and Y. C. Lin, Phys. Rev. D **37**, 2423 (1989).
[37] J. Bijnens and F. Cornet, Nucl. Phys. **B296**, 557 (1988).
[38] S. Egli *et al.*, Phys. Lett. B **175**, 97 (1986).
[39] M. Moreno and J. Pestieau, Phys. Rev. D **13**, 175 (1976); C. Y. Lee, *ibid.* **32**, 658 (1985).
[40] S. B. Gerasimov, Yad. Fiz. **29**, 513 (1979) [Sov. J. Nucl. Phys. **29**, 259 (1979)].
[41] N. Paver and M. D. Scadron, Nuovo Cimento **78A**, 159 (1983).
[42] B. R. Holstein, Phys. Rev. D **33**, 3316 (1986); J. F. Donoghue, C. Ramirez, and G. Valencia, *ibid.* **39**, 1947 (1989).